On the complete radiation-diffraction problem and wave-drift damping of marine bodies in the yaw mode of motion

by

Styrk Finne and John Grue

Mechanics Division, Department of Mathematics,
University of Oslo, Norway

Abstract

The coupled radiation-diffraction problem due to a floating body with slow (time-dependent) rotation about the vertical axis in incoming waves is studied by means of potential theory. The water depth may be finite. First, the radiation problem is considered. It is shown how the various components of the velocity potential may be obtained by means of integral equations. The first order forces in the coupled radiation-diffraction problem are then considered. Generalized Haskind relations for the exciting forces and generalized Timman-Newman relations for the added mass and damping forces are deduced for bodies of arbitrary shape with vertical walls at the water line. The equation of motion is obtained, and the frequencies of the linear body responses superposed on the slow rotation are identified. Formulae for the wave drift damping coefficients in the yaw mode of motion are derived on explicit form, and the energy equation is discussed. Computations illustrating the various aspects of the method are performed for two ships. The wave drift damping moment is found to become positive in the present cases.

1 Introduction

The coupled radiation-diffraction problem due to a floating body moving with a slow rotation about the vertical axis in monochromatic waves is considered. The paper is complementary to the work by Grue and Palm (1996) who described the corresponding diffraction problem. The radiation problem is outlined in the first few sections of the paper. In this case, a body is performing (forced) small oscillations in six degrees of freedom superimposed on a slow rotation about the vertical axis in the surface of an otherwise calm fluid. The coupled radiation-diffraction problem is next considered, as we derive formulae for the induced hydrodynamical forces and the equation of motion determining the linear body responses. The ultimate goal is to describe the remaining parts of a method to obtain the three by three wave drift damping matrix of a floating body of general shape, including the complete radiation-diffraction effects.

The study is motivated by needs in the offshore industry to describe wave induced forces and motions of moored production ships and floating oil platforms. Such production systems may be lightly moored and may experience slow motions with large amplitudes in the horizontal plane. These motions are excited by nonlinear loads due to wind, current and waves, and have periods determined by the mass and spring properties of the moored body. They are limited by hydrodynamical damping forces, where wave drift damping has proved to give important contribution.

The notion of wave drift damping was introduced by Wichers and van Sluijs (1979) who performed decaying tests of moored tankers in waves. Rational theories were after some while derived, enabling evaluation of wave drift damping due to a slow translation, by Zhao and Faltinsen (1989), Nossen, Grue and Palm (1991), Grue and Palm (1993) for bodies of arbitrary shape, by Emmerhoff and Sclavounos (1992), Malenica, Clark and Molin (1995) for vertical circular cylinders. Later, wave drift damping due to a slow rotation was accounted for by Newman (1993), who also considered the complete wave drift damping matrix, and by Grue and Palm (1996). The latter two works allow for arbitrary geometries, but the problem is simplified by considering only the diffraction part of the linear wave field. Wave drift damping in the yaw mode of motion is also described for vertical circular cylinders by Emmerhoff and Sclavounos (1996).

In the present work we describe the complete radiation-diffraction problem of a floating body of arbitrary shape rotating slowly about the vertical axis, generalizing the method by Grue and Palm (1996), hereinafter referred to as GP. We apply potential theory to describe the motion of an incompressible and homogeneous fluid, as viscous effects are disregarded (§§2-3). The water depth may be finite in all derivations. Applying perturbation expansions in the wave amplitude and the slow angular velocity we decompose the velocity potential, deriving a set of boundary value problems for its various components. Among some new features in the radiation problem coupled with a slow yaw velocity of the body, the usual m_j-terms include in the present formulation some new components. The coupling between the slow motion and steady second order velocities in the fluid is consistently accounted for (§4). The boundary value problems are solved by means of integral equations involving unknown quantities on the wetted body surface only (§5). The method requires evaluation of ordinary integrals over the mean free surface, which have relatively quick convergence and are relatively robust to evaluate.

In §6 the first order forces and motions of the body are considered. Several results costumary in the case of unidirectional motion of a body in waves may be generalized to the case of a slow rotation of the body, still allowing for a general shape of the geometry, except for a requirement of vertical walls at the water line of the body. Thus we deduce generalized Haskind relations for the exciting forces and generalize the Timman-Newman relations for the added mass and damping forces to the present case. Numerical results confirm these relations. The equation of motion determining the linear responses of the body is derived, accounting for the Coriolis force. We also identify the frequencies of the linear body responses which are superimposed on the slow rotation, finding that the different modes of motion may in general have different frequencies. Furthermore, the frequency of the motion may differ from the frequency of the exciting force in the respective modes.

Formulae on explicit form for the wave drift damping coefficients due to the slow rotation (§7) are derived using conservation of linear and angular momentum. The derivations in the coupled radiation-diffraction problem become somewhat more complex than when there are no body responses. The resulting formulae are compared with the diffraction analyses by Newman (1993), GP and Grue (1996). Wave drift damping computations are performed for two ships. Various aspects of the method are discussed in §8, including convergence and the energy balance. The convergence tests indicate that the linear forces and motions, the time-averaged second order forces and the wave drift damping matrix may be obtained with a relative accuracy within a few percents, depending on the discretization of the geometry.

For a slow rotation about a vertical axis far away from the body we recover results due to a slow unidirectional motion. In this connection, it is relevant to compare with some recent formulae on the translatory problem proposed by Aranha (1996). We find here in general poor agreement between the present and his method, both for the linear and second order parts of the problem. The only exceptions are the wave drift damping in unidirectional motion of a floating hemisphere and an array of restrained vertical circular cylinders; the details are explained in §8.2. Finally, §9 is a conclusion.

2 Mathematical formulation

We consider a floating body moving with a slow yaw-velocity (rotation about the vertical axis) while responding to incoming monochromatic waves. We define a fixed frame of reference and a relative frame of reference where the latter follows the slow motion of the body, which is rotated an angle α relative to the fixed frame of reference. A coordinate system $O - xyz$ is introduced in the relative frame of reference with the xy-plane in the mean free surface of the fluid and the z-axis being vertical upwards. Unit vectors $\mathbf{i}, \mathbf{j}, \mathbf{k}$ are introduced accordingly. The angular velocity is denoted by $\Omega\mathbf{k} = \dot{\alpha}\mathbf{k}$, where a dot denotes time derivative.

We shall throughout the paper consider the problem in the relative frame of reference. The incoming waves described in this frame of reference are determined by the potential

$$\Phi^I = Re[(Aig/\omega)\phi^I e^{i\omega t}], \qquad \phi^I = Ch(kz)e^{-ikR\cos(\beta-\theta)}, \tag{1}$$

where $Ch(kz) \equiv \cosh k(z+h)/\cosh kh$, and A, k and ω denote amplitude, wavenumber and frequency, respectively, of the incoming waves, h the water depth, and g the acceleration due to gravity. ω and k obey the dispersion relation

$$K = k\tanh kh, \quad \text{where} \quad K = \omega^2/g \tag{2}$$

The wave angle β is defined as the angle between the positive x-axis and the wave direction. In (1) we have also introduced polar coordinates by $x = R\cos\theta$, $y = R\sin\theta$.

The slow rotation of the body introduces effectively a slowly varying wave angle to an observer in the relative frame of reference. This is determined by $\beta(t) + \alpha(t) = \beta_0$, which means that $d\beta/dt = -\Omega$. (β_0 is the wave angle in the fixed frame of reference.) We let the rotation angle α be arbitrary and the non-dimensional wavenumber kl be of order one, where l denotes the characteristic length of the body. We assume, however, that Ω is small compared to the wave frequency. Introducing the small parameter $\epsilon = \Omega/\omega$ we shall in the mathematical analysis apply perturbation expansions in A/l and ϵ, retaining terms up to order $(A/l)^2$ and ϵ. (This means e.g. that terms proportional to $\dot{\Omega}/\omega^2 = O(\epsilon^2)$ are neglected.) The perturbed problem then has two time-scales, a fast time-scale with characteristic time $1/\omega$ and a slow time-scales with characteristic time $1/\Omega$. To obtain the wave drift damping, a time-average over the fast time-scale is applied.

Let $\mathbf{v}$ denote the fluid velocity in the relative frame of reference. This may be decomposed by $\mathbf{v} = \nabla\Phi' - \Omega\mathbf{k} \times \boldsymbol{x}$, where Φ' is a velocity potential and $-\Omega\mathbf{k} \times \boldsymbol{x}$ denotes the velocity introduced to an observer moving from the fixed to the relative frame of reference. The potential Φ' satisfies the Laplace equation since $\nabla \cdot \mathbf{v} = 0$, according to the assumptions. We decompose Φ' by $\Phi' = \Omega\chi_6 + \Phi + \psi^{(2)}$, where $\Omega\chi_6$ denotes the potential due to the flow generated by the body when there are no waves, Φ the linear wave potential being proportional to the wave amplitude and is due to the incoming, scattered and radiated waves, and $\psi^{(2)}$ the time-averaged potential being proportional to the wave amplitude squared. It is convenient to introduce $\mathbf{w} = -\mathbf{k} \times \boldsymbol{x} + \nabla\chi_6$, where $\mathbf{w}$ satisfies the rigid wall condition at the body, at the free surface and at the sea floor. Furthermore, $\nabla\chi_6$ vanishes for $R \to \infty$.

3 The boundary conditions for Φ

3.1 The free surface boundary condition

The free surface boundary condition for Φ is obtained by applying the individual derivative to the Bernoulli equation for the pressure at the free surface. After linearizing with respect to the wave amplitude, we find (see GP §3)

$$\frac{\partial^2\Phi}{\partial t^2} + 2\Omega\mathbf{w}\cdot\nabla_h\frac{\partial\Phi}{\partial t} + \Omega\frac{\partial\Phi}{\partial t}\nabla_h\cdot\mathbf{w} + g\frac{\partial\Phi}{\partial z} = 0 \text{ at } z = 0, \tag{3}$$

where ∇_h denotes the horizontal gradient. We next introduce the decomposition of Φ as follows

$$\Phi = Re\Big\{\frac{iAg}{\omega}\phi_D e^{i\omega t} + \sum_{j=1}^{6}\frac{d}{dt}\Big(\xi_j e^{i\omega t}\Big)\phi_j\Big\} \tag{4}$$

where the first part represents the incoming and scattered waves, and the second part the radiation potentials. ξ_j are the linear responses, see (16).

We here consider the radiation potentials. The corresponding diffraction potential and its decomposition were described by GP; a short account is given in Appendix A. As already noted, the motion in the relative frame of reference depend on the slowly varying wave angle $\beta(t)$. To first order in ϵ we then have

$$\frac{d}{dt}(\xi_j e^{i\omega t}) = \Big(i\omega\xi_j + \frac{d\xi_j}{dt}\Big)e^{i\omega t} = i\omega\Big(\xi_j + i\epsilon\frac{\partial\xi_j}{\partial\beta}\Big)e^{i\omega t}, \quad j = 1,...6 \tag{5}$$

where we have exploited that $d\beta/dt = -\Omega$. We may show that $\partial\phi_j/\partial t = O(\epsilon^2)$ for $j = 1,...6$, see the comments on the last two lines of §3.2. Inserting (4)–(5) into (3) and retaining terms up to first order in ϵ, we obtain

$$-K\Big(\xi_j + 3i\epsilon\frac{\partial\xi_j}{\partial\beta}\Big)\phi_j + i\epsilon K\xi_j(2\mathbf{w}\cdot\nabla_h\phi_j + \phi_j\nabla_h\cdot\mathbf{w}) + \Big(\xi_j + i\epsilon\frac{\partial\xi_j}{\partial\beta}\Big)\frac{\partial\phi_j}{\partial z} = 0 \tag{6}$$

at $z = 0$, where sum over j is understood. It is now convenient to introduce perturbation expansions for ξ_j and $\xi_j\phi_j$. The boundary condition (6) suggests expansions as follows

$$\xi_j = \xi_j^0 + \epsilon\xi_j^1, \quad j = 1,...6 \tag{7}$$

$$\xi_j\phi_j = \xi_j^0\phi_j^0 + \epsilon\Big(\xi_j^1\phi_j^0 + (\partial\xi_j^0/\partial\beta)\phi_j^{11} + \xi_j^0\psi_j^1\Big) \tag{8}$$

where the potentials ϕ_j^{11} and ψ_j^1 are specified below. To order ϵ^0 we then obtain

$$-K\phi_j^0 + \frac{\partial\phi_j^0}{\partial z} = 0 \quad \text{at} \quad z = 0 \tag{9}$$

To order ϵ^1 we find

$$-K\Big\{\Big(\xi_j^1\phi_j^0 + \xi_j^0\psi_j^1 + \frac{\partial\xi_j^0}{\partial\beta}\Big(\phi_j^{11} + 3i\phi_j^0\Big)\Big\} + iK\xi_j^0(2\mathbf{w}\cdot\nabla_h\phi_j^0 + \phi_j^0\nabla_h\cdot\mathbf{w})$$
$$+\Big\{\xi_j^1\frac{\partial\phi_j^0}{\partial z} + \xi_j^0\frac{\partial\psi_j^1}{\partial z} + \frac{\partial\xi_j^0}{\partial\beta}\Big(\frac{\partial\phi_j^{11}}{\partial z} + i\frac{\partial\phi_j^0}{\partial z}\Big)\Big\} = 0 \quad \text{at} \quad z = 0 \tag{10}$$

Exploiting (9), this gives

$$-K\phi_j^{11} + \frac{\partial\phi_j^{11}}{\partial z} = 2iK\phi_j^0 \quad \text{at} \quad z = 0 \tag{11}$$

$$-K\psi_j^1 + \frac{\partial\psi_j^1}{\partial z} = 2iK\frac{\partial\phi_j^0}{\partial\theta} - 2iK\nabla_h\phi_j^0\cdot\nabla\chi_6 - iK\phi_j^0\nabla_h^2\chi_6 \quad \text{at} \quad z = 0 \tag{12}$$

for $j = 1, ...6$. In the far-field analysis carried out later, among others to obtain the wave drift damping coefficients, it is convenient to decompose ψ_j^1 into $\psi_j^1 = \phi_j^{12} + \phi_j^{13}$, where ϕ_j^{12} and ϕ_j^{13} at the free surface satisfy

$$-K\phi_j^{12} + \frac{\partial \phi_j^{12}}{\partial z} = 2iK\frac{\partial \phi_j^0}{\partial \theta} \quad \text{at} \quad z = 0 \tag{13}$$

$$-K\phi_j^{13} + \frac{\partial \phi_j^{13}}{\partial z} = -2iK\nabla_h \phi_j^0 \cdot \nabla \chi_6 - iK\phi_j^0 \nabla_h^2 \chi_6 \quad \text{at} \quad z = 0 \tag{14}$$

for $j = 1, ...6$. The potentials ϕ_j^{11} and ϕ_j^{12} may be expressed in terms of ϕ_j^0 by

$$\phi_j^{11} = 2iK\frac{\partial \phi_j^0}{\partial K}, \qquad \phi_j^{12} = 2iK\frac{\partial^2 \phi_j^0}{\partial K \partial \theta} \tag{15}$$

3.2 The boundary condition at the body

We next consider the kinematic boundary condition at the surface of the body. The linear body motions are determined by

$$\tilde{\mathbf{B}} = \tilde{\boldsymbol{\xi}} + \tilde{\boldsymbol{\alpha}} \times \boldsymbol{x} \tag{16}$$

where $\tilde{\boldsymbol{\xi}} = Re\{(\xi_1, \xi_2, \xi_3)e^{i\omega t}\}$ and $\tilde{\boldsymbol{\alpha}} = Re\{(\xi_4, \xi_5, \xi_6)e^{i\omega t}\}$ denote respectively the first order translations and rotations. We note that frequencies of the body oscillations in general differ from ω when $\Omega \neq 0$, see §6.4. The kinematic boundary condition gives

$$\mathbf{N} \cdot \{\Omega \mathbf{w} + \nabla \Phi + \nabla \psi^{(2)}\} = \mathbf{N} \cdot d\tilde{\mathbf{B}}/dt \tag{17}$$

which applies at the instantaneous position of the body, and where $\mathbf{N}$ denotes the instantaneous unit normal vector, pointing out of the fluid. We then expand (17) about the mean position of the body, which we denote by S_B. The normal vector $\mathbf{N}$ may be expressed by

$$\mathbf{N} = \mathbf{n} + \tilde{\boldsymbol{\alpha}} \times \mathbf{n} \tag{18}$$

where $\mathbf{n} = (n_1, n_2, n_3)$ denotes the unit normal vector when $\tilde{\boldsymbol{\alpha}} = 0$. After expanding the parenthesis in (17) we find

$$(\mathbf{n} + \tilde{\boldsymbol{\alpha}} \times \mathbf{n}) \cdot \{\Omega \mathbf{w} + \nabla \Phi + \nabla \psi^{(2)} + \tilde{\mathbf{B}} \cdot \nabla(\Omega \mathbf{w} + \nabla \Phi)\} = (\mathbf{n} + \tilde{\boldsymbol{\alpha}} \times \mathbf{n}) \cdot d\tilde{\mathbf{B}}/dt \tag{19}$$

where terms proportional to $O(A^3, \epsilon A^2, \epsilon^2)$ are omitted. For the terms in (19) proportional to $e^{i\omega t}$ we find

$$\mathbf{n} \cdot \nabla \Phi + \Omega[(\tilde{\boldsymbol{\alpha}} \times \mathbf{n}) \cdot \mathbf{w} + \mathbf{n} \cdot (\tilde{\mathbf{B}} \cdot \nabla \mathbf{w})] = \mathbf{n} \cdot d\tilde{\mathbf{B}}/dt \tag{20}$$

We then utilize the vector relation

$$\mathbf{n} \cdot (\tilde{\mathbf{B}} \cdot \nabla \mathbf{w}) = (\tilde{\mathbf{B}} \times \mathbf{n}) \cdot (\nabla \times \mathbf{w}) + \tilde{\mathbf{B}} \cdot \partial \mathbf{w}/\partial n \tag{21}$$

and, furthermore,

$$\tilde{\mathbf{B}} \cdot \frac{\partial \mathbf{w}}{\partial n} = \tilde{\boldsymbol{\xi}} \cdot \frac{\partial \mathbf{w}}{\partial n} + \tilde{\boldsymbol{\alpha}} \cdot \frac{\partial}{\partial n}(\boldsymbol{x} \times \mathbf{w}) - (\tilde{\boldsymbol{\alpha}} \times \mathbf{n}) \cdot \mathbf{w} \tag{22}$$

In our case, $\mathbf{w}$ has nonzero vorticity, given by

$$\nabla \times \mathbf{w} = -2\mathbf{k} \tag{23}$$

Combining (20)–(22) we find

$$\mathbf{n}\cdot\nabla\Phi = \mathbf{n}\cdot\frac{d}{dt}(\tilde{\boldsymbol{\xi}}+\tilde{\boldsymbol{\alpha}}\times\boldsymbol{x}) - \Omega\Big\{\tilde{\boldsymbol{\xi}}\cdot(\frac{\partial\mathbf{w}}{\partial n}+2\mathbf{k}\times\mathbf{n})+\tilde{\boldsymbol{\alpha}}\cdot\Big[\frac{\partial}{\partial n}(\boldsymbol{x}\times\mathbf{w})+2\boldsymbol{x}\times(\mathbf{k}\times\mathbf{n})\Big]\Big\} \quad (24)$$

We then insert (4), (5), (7) and (8) into (24) and obtain

$$\frac{\partial\phi_j^0}{\partial n} = n_j, \quad j=1,...6 \quad \text{at } S_B \quad (25)$$

where $(n_4, n_5, n_6) = \boldsymbol{x}\times\mathbf{n}$,

$$\frac{\partial\phi_j^{11}}{\partial n} = 0, \quad j=1,...6 \quad \text{at } S_B \quad (26)$$

$$\frac{\partial\psi_j^1}{\partial n} = -im_j, \quad j=1,...6 \quad \text{at } S_B \quad (27)$$

Here, generalized m_j-terms are determined by

$$(m_1, m_2, m_3) = -\frac{\partial\mathbf{w}}{\partial n} - 2\mathbf{k}\times\mathbf{n} \quad (28)$$

$$(m_4, m_5, m_6) = -\frac{\partial}{\partial n}(\boldsymbol{x}\times\mathbf{w}) - 2\boldsymbol{x}\times(\mathbf{k}\times\mathbf{n}) \quad (29)$$

Thus, m_j contain in the present problem the extra terms $-2\mathbf{k}\times\mathbf{n}$ and $-2\boldsymbol{x}\times(\mathbf{k}\times\mathbf{n})$ due to the rotation of the body. These terms are absent for bodies with translatory motion in waves.

We note that the boundary conditions for ϕ_j^0, ϕ_j^{11} and ψ_j^1 do not depend on the wave angle β, which means that these potentials do not depend on β.

3.3 The boundary condition at the sea floor

At the seafloor all the potentials satisfy the rigid wall condition, i.e.

$$\frac{\partial}{\partial n}(\text{potential}) = 0 \quad \text{at} \quad z=-h \quad (30)$$

3.4 The potentials in the far-field

The potential $\Phi - \Phi^I$ is generated by the presence of the floating body, and represents outgoing waves at some distance from the body. The far-field forms of the potentials ϕ_j^0 and ϕ_j^{13} become

$$\phi_j^0 = R^{-1/2}H_j^0(\theta)Ch(kz)e^{-ikR}(1+O((kR)^{-1})), \quad j=1,...6 \quad (31)$$

$$\phi_j^{13} = R^{-1/2}H_j^{13}(\theta)Ch(kz)e^{-ikR}(1+O((kR)^{-1})), \quad j=1,...6 \quad (32)$$

where H_j^0 and H_j^{13} are determined below by (60) and (61), respectively. For ϕ_j^{11} and ψ_j^1 we may, using (31) and (32), show that

$$\frac{\partial\phi_j^{11}}{\partial R} = -ik\phi_j^{11} + \phi_j^0 + O((kR)^{-3/2}) \quad j=1,...6 \quad (33)$$

$$\frac{\partial\psi_j^1}{\partial R} = -ik\psi_j^1 + \frac{\partial\phi_j^0}{\partial\theta} + O((kR)^{-3/2}) \quad j=1,...6 \quad (34)$$

Similar relations may be derived for the various components of the diffraction potential ϕ_D^1, see Appendix A. We may for finite value of R apply (33) and (34) in the far-field analysis, since all terms of the expansion of the potential in principle are included. In deriving integral equations for the potentials and formulae for the forces and moments, we shall integrate the potentials at a control surface for large, but finite R. We remark that the terms proportional to $R^{1/2}e^{-ikR}$ in ϕ_j^{11}, ψ_j^1 (and ϕ_D^1) always disappear in these formulae, which means that we may let $R \to \infty$ to obtain the final results.

For later use we write the complete radiation-diffraction potential Φ as follows

$$\Phi = Re\Big(\frac{iAg}{\omega}(\phi^0 + \epsilon\phi^1 + ...)e^{i\omega t}\Big) \tag{35}$$

where

$$\phi^0 = \phi_D^0 + K(\xi_j^0/A)\phi_j^0 \tag{36}$$

$$\phi^1 = 2iK\frac{\partial^2\phi^0}{\partial K\partial\beta} + 2iK\frac{\partial^2\phi^0}{\partial K\partial\theta} + \phi^{13} \tag{37}$$

$$\phi^{13} = \phi_7^{13} + K\Big[\Big(\xi_j^1 + i\frac{\partial\xi_j^0}{\partial\beta} - 2i\frac{\partial^2(K\xi_j^0)}{\partial K\partial\beta}\Big)\phi_j^0 - 2i\frac{\partial(K\xi_j^0)}{\partial K}\frac{\partial\phi_j^0}{\partial\theta} + \xi_j^0\phi_j^{13}\Big]/A \tag{38}$$

In the far-field we then have

$$\phi^0 - \phi^I = R^{-1/2}H^0(\theta)Ch(kz)e^{-ikR}(1 + O((kR)^{-1})) \tag{39}$$

$$\phi^{13} = R^{-1/2}H^{13}(\theta)Ch(kz)e^{-ikR}(1 + O((kR)^{-1})) \tag{40}$$

where

$$H^0 = H_7^0 + K\xi_j^0H_j^0/A \tag{41}$$

$$H^{13} = H_7^{13} + K\Big[\Big(\xi_j^1 + i\frac{\partial\xi_j^0}{\partial\beta} - 2i\frac{\partial^2(K\xi_j^0)}{\partial K\partial\beta}\Big)H_j^0 - 2i\frac{\partial(K\xi_j^0)}{\partial K}\frac{\partial H_j^0}{\partial\theta} + \xi_j^0H_j^{13}\Big]/A \tag{42}$$

The amplitudes H_7^0 and H_7^{13} are given in (139) and (140), respectively.

4 The potential $\psi^{(2)}$

The second order potential $\psi^{(2)}$ appears in the formulae for the time-averaged pressure, force and moment always multiplied by Ω, and it suffices to consider the boundary value problem for $\psi^{(2)}$ when $\Omega = 0$, to leading order. The free surface boundary condition for $\psi^{(2)}$ then reads

$$\frac{\partial\psi^{(2)}}{\partial z} = -\frac{A^2g}{2\omega}Im\Big(\phi^0\frac{\partial^2\phi^{0*}}{\partial z^2}\Big) \quad \text{at } z = 0 \tag{43}$$

where a star denotes complex conjugate. The boundary condition at S_B is obtained from the time-averaged part of (20), giving

$$\frac{\partial\psi^{(2)}}{\partial n} = \frac{A^2g}{2\omega}Im\{\mathbf{B}^0\cdot(\mathbf{n}\cdot\nabla)\nabla\phi^{0*} - \mathbf{C}^0\cdot(K\mathbf{B}^{0*} - \nabla\phi^{0*})\} \quad \text{at } S_B \tag{44}$$

where

$$\mathbf{B}^0 = [(\xi_1^0, \xi_2^0, \xi_3^0) + (\xi_4^0, \xi_5^0, \xi_6^0)\times\boldsymbol{x}]/A, \qquad \mathbf{C}^0 = (\xi_4^0, \xi_5^0, \xi_6^0)\times\mathbf{n}/A \tag{45}$$

A complete discussion of how to obtain $\psi^{(2)}$ is given in Grue and Palm (1993).

5 Integral equations

5.1 The potentials ϕ_j^0 and their derivatives

To solve the boundary value problems for ϕ_j^0 we first introduce a Green function, $G^0(x',y',z',x,y,z)$, being a sink at $\boldsymbol{x}=\boldsymbol{x}'=(x',y',z')$, satisfying the free surface boundary condition (9). This Green function may be found in e.g. Wehausen and Laitone (1960, eq. 13.18). By applying Green's theorem to ϕ_j^0 and G^0 it may be shown that ϕ_j^0 in the radiation problem satisfies

$$\int_{S_B}\left(\phi_j^0\frac{\partial G^0}{\partial n}-G^0 n_j\right)dS=\left\{\begin{array}{ll}-2\pi\phi_j^0(\boldsymbol{x}) & \boldsymbol{x}\in S_B\\ -4\pi\phi_j^0(\boldsymbol{x}) & \boldsymbol{x}\in\mathcal{V}\end{array}\right. \quad j=1,...6 \tag{46}$$

Here, $\mathcal{V}$ denotes the fluid volume enclosed by the body surface, S_B, the free surface, S_F, and the vertical circular cylinder, S_R, with finite radius R, and the first case is an integral equation for ϕ_j^0.

The various derivatives of the potential ϕ_j^0 may be obtained by means of integral equations. By differentiating (46) with respect to K, we obtain that $\partial\phi_j^0/\partial K$ is determined by

$$\int_{S_B}\left(\phi_{j,K}^0\frac{\partial G^0}{\partial n}+\phi_j^0\frac{\partial^2 G^0}{\partial n\partial K}-\frac{\partial G^0}{\partial K}n_j\right)dS=\left\{\begin{array}{ll}-2\pi\phi_{j,K}^0(\boldsymbol{x}) & \boldsymbol{x}\in S_B\\ -4\pi\phi_{j,K}^0(\boldsymbol{x}) & \boldsymbol{x}\in\mathcal{V}\end{array}\right. \quad j=1,...6 \tag{47}$$

where $\phi_{i,K}^0\equiv\partial^2\phi_j^0/\partial K$. By multiplying $\phi_{j,K}^0$ by $2iK$ we obtain ϕ_j^{11} $(j=1,...6)$.

The potential $\partial^2\phi_j^0/\partial\theta\partial K$ is determined by differentiating (47) with respect to the θ-variable, i.e.

$$\int_{S_B}\left(\phi_{j,K}^0\frac{\partial^2 G^0}{\partial\theta\partial n}dS+\phi_j^0\frac{\partial^3 G^0}{\partial K\partial\theta\partial n}-\frac{\partial^2 G^0}{\partial K\partial\theta}n_j\right)dS=-4\pi\phi_{j,\theta K}^0(\boldsymbol{x}),\ \ \boldsymbol{x}\in\mathcal{V},\ \ j=1,...6 \tag{48}$$

which, multiplied by $2iK$, determines ϕ_j^{12} for $\boldsymbol{x}\in\mathcal{V}$.

5.2 The potential ψ_j^1

Due to the boundary condition (27) at S_B, it is more convenient to derive an integral equation for the sum $\psi_j^1=\phi_j^{12}+\phi_j^{13}$ at S_B than for the potential ϕ_j^{13}. We then first apply Green's theorem to ψ_j^1 and G^0, giving

$$\int_{S_B}\left(\psi_j^1\frac{\partial G^0}{\partial n}-G^0\frac{\partial\psi_j^1}{\partial n}\right)dS+\int_{S_F+S_R}\left(\psi_j^1\frac{\partial G^0}{\partial n}-G^0\frac{\partial\psi_j^1}{\partial n}\right)dS=\left\{\begin{array}{ll}-2\pi\psi_j^1(\boldsymbol{x}) & \boldsymbol{x}\in S_B\\ -4\pi\psi_j^1(\boldsymbol{x}) & \boldsymbol{x}\in\mathcal{V}\end{array}\right. \tag{49}$$

By applying the free surface boundary conditions for ψ_j^1 and G^0 (see (12) and (9), respectively), (49) reduces to

$$\int_{S_B}\left(\psi_j^1\frac{\partial G^0}{\partial n}-G^0\frac{\partial\psi_j^1}{\partial n}\right)dS+2iK\int_{S_F}G^0\left(-\frac{\partial\phi_j^0}{\partial\tilde\theta}+\nabla_h\phi_j^0\cdot\nabla_h\chi_6+\frac{1}{2}\phi_j^0\nabla_h^2\chi_6\right)dS$$
$$+\int_{S_R}\left(\psi_j^1\frac{\partial G^0}{\partial n}-G^0\frac{\partial\psi_j^1}{\partial n}\right)dS=\left\{\begin{array}{ll}-2\pi\psi_j^1(\boldsymbol{x}) & \boldsymbol{x}\in S_B\\ -4\pi\psi_j^1(\boldsymbol{x}) & \boldsymbol{x}\in\mathcal{V}\end{array}\right. \tag{50}$$

Following GP, we introduce an auxiliary function $G^1=2iK\partial^2G^0/\partial\tilde\theta\partial K$, where $\tilde\theta$ is defined by $x'=\tilde R\cos\tilde\theta$, $y'=\tilde R\sin\tilde\theta$, $\tilde R^2=x'^2+y'^2$. Applying Green's theorem to ϕ_j^0 and G^1, and introducing the boundary conditions for ϕ_j^0 and G^0 at the free surface, we obtain

$$\int_{S_B}\left(\phi_j^0\frac{\partial G^1}{\partial n}-G^1\frac{\partial\phi_j^0}{\partial n}\right)dS+2iK\int_{S_F}\phi_j^0\frac{\partial G^0}{\partial\tilde{\theta}}dS+\int_{S_R}\left(\phi_j^0\frac{\partial G^1}{\partial n}-G^1\frac{\partial\phi_j^0}{\partial n}\right)dS=0 \quad (51)$$

Subtracting (51) from (50) gives

$$\begin{aligned}&\int_{S_B}\left(\psi_j^1\frac{\partial G^0}{\partial n}-G^0\frac{\partial\psi_j^1}{\partial n}-\phi_j^0\frac{\partial G^1}{\partial n}+G^1\frac{\partial\phi_j^0}{\partial n}\right)dS\\&+2iK\int_{S_F}\left(-\frac{\partial}{\partial\tilde{\theta}}(G^0\phi_j^0)+G^0(\nabla_h\phi_j^0\cdot\nabla_h\chi_6+\frac{1}{2}\phi_j^0\nabla_h^2\chi_6)\right)dS\\&+\int_{S_R}\left(\psi_j^1\frac{\partial G^0}{\partial n}-G^0\frac{\partial\psi_j^1}{\partial n}-\phi_j^0\frac{\partial G^1}{\partial n}+G^1\frac{\partial\phi_j^0}{\partial n}\right)dS=\begin{cases}-2\pi\psi_j^1(\boldsymbol{x}) & \boldsymbol{x}\in S_B\\-4\pi\psi_j^1(\boldsymbol{x}) & \boldsymbol{x}\in\mathcal{V}\end{cases}\end{aligned} \quad (52)$$

We note that ψ_j^1 and G^1 satisfy the same condition at S_R, see eq. (34). By applying this condition together with the far-field condition (31) for ϕ_j^0 and G^0, and then applying partial integration with respect to the $\tilde{\theta}$–variable, we find that the integral over S_R vanishes for $R\to\infty$. The integral over S_F in (52) may be further developed, and after some algebra we find for this integral

$$-\int_{S_F}\phi_j^0 L_h(G^0,\chi_6)dS \quad (53)$$

where

$$L_h(G^0,\chi_6)=2iK\nabla_h G^0\cdot\nabla_h\chi_6+iKG^0\nabla_h^2\chi_6 \quad (54)$$

We then apply the boundary conditions for ϕ_j^0 and ψ_j^1 at S_B, (25) and (27), respectively. The latter boundary condition leads to integrals over the m_j-terms. These require evaluation of the derivative of $\mathbf{w}$ along the normal of S_B, and are not on a suitable form. However, by using a variant of Stokes theorem, and applying the properties of $\mathbf{w}$, where $\nabla\times\mathbf{w}$ is nonzero, we may rewrite these integrals by

$$\int_{S_B}G^0 m_j dS=-\int_{S_B}\mathbf{w}\cdot\nabla G^0 n_j dS \quad (55)$$

Thus, (52) becomes

$$\int_{S_B}\left(\psi_j^1\frac{\partial G^0}{\partial n}-i\mathbf{w}\cdot\nabla G^0 n_j-\phi_j^0\frac{\partial G^1}{\partial n}+G^1 n_j\right)dS-\int_{S_F}\phi_j^0 L_h(G^0,\chi_6)dS=\begin{cases}-2\pi\psi_j^1(\boldsymbol{x}) & \boldsymbol{x}\in S_B\\-4\pi\psi_j^1(\boldsymbol{x}) & \boldsymbol{x}\in\mathcal{V}\end{cases} \quad (56)$$

for $j=1,...6$, where the first case is an integral equation for ψ_j^1.

The integral equations for the various potentials are solved by means of a low-order panel method, where the geometry is discretized by means of quadrilaterals. The most important numerical aspects of the method are commented on in Appendix B.

5.3 Far-field amplitudes

We are now able to determine the far-field amplitudes of the potentials ϕ_j^0 and ϕ_j^{13}, see (31)–(32). First we note that the far-field form of G^0 reads

$$G^0=R^{-1/2}h^0(\theta,\boldsymbol{x}')Ch(kz)e^{-ikR}(1+O((kR^{-1}))) \quad (57)$$

where

$$h^0 = \frac{\sqrt{2\pi k}}{C_g(kh)}\Big(\tanh kh + 1\Big)\Big(e^{kz'} + e^{-k(z'+2h)}\Big)e^{k(ix'\cos\theta + iy'\sin\theta) - i\pi/4} \tag{58}$$

and

$$C_g(kh) = \tanh kh + \frac{kh}{\cosh^2 kh} \equiv \frac{\partial\omega/\partial k}{g/2\omega}. \tag{59}$$

(C_g denotes the ratio between the group velocity of a wave with frequency ω at finite and infinite water depth, respectively.) The far-field amplitude H_j^0 is obtained by inserting the far-field form of G^0 into (46), i.e.

$$4\pi H_j^0(\theta) = -\int_{S_B} (\phi_j^0 \frac{\partial h^0}{\partial n} - h^0 n_j) dS \tag{60}$$

The far-field amplitude H_j^{13} is obtained by first subtracting (48) multiplied by $2iK$ from (56) and then using (57), giving

$$4\pi H_j^{13}(\theta) = -\int_{S_B} (\psi_j^1 \frac{\partial h^0}{\partial n} - 2iK\phi_{j,K}^0 \frac{\partial^2 h^0}{\partial\theta\partial n} - i\nabla h^0 \cdot \mathbf{w} n_j) dS + \int_{S_F} \phi_j^0 L_h(h^0, \chi_6) dS \tag{61}$$

6 First order forces and body responses

6.1 Exciting forces and generalized Haskind relations

An expression for the pressure in a rotating frame of reference was derived by GP, eq. (2.7). From this we find that the linear dynamic pressure reads $p = -\rho(\partial\Phi/\partial t + \Omega\mathbf{w}\cdot\nabla\Phi)$, where ρ denotes the density of the fluid. The linear exciting forces and moments are obtained by integrating the pressure over the body surface. By setting $\xi_j = 0$ ($j = 1, ...6$) in Φ we obtain

$$\begin{aligned} F_i^{ex} &= -\rho \int_{S_B} \Big(\frac{\partial\Phi}{\partial t} + \Omega\mathbf{w}\cdot\nabla\Phi\Big) n_i dS \\ &= \rho g A Re\Big\{e^{i\omega t}\Big(\int_S \phi_D^0 n_i dS + \epsilon\int_S (i\frac{\partial\phi_D^0}{\partial\beta} + \phi_D^1 - \mathbf{w}\cdot\nabla\phi_D^0) n_i dS\Big)\Big\}, \quad i = 1, ...6 \end{aligned} \tag{62}$$

Introducing

$$X_i^0 = \rho g \int_{S_B} \phi_D^0 n_i dS, \qquad X_i^1 = \rho g \int_{S_B} (\phi_D^1 - i\mathbf{w}\cdot\nabla\phi_D^0) n_i dS \tag{63}$$

we may write

$$F_i^{ex} = A\, Re\Big\{\Big(X_i^0 + \epsilon(i\frac{\partial X_i^0}{\partial\beta} + X_i^1)\Big)e^{i\omega t}\Big\} \tag{64}$$

The exciting forces may, when $\Omega = 0$, be found from the Haskind relations, which in one form expresses X_i^0 in terms of the far-field amplitude of ϕ_i^0 (see e.g. Newman 1977 §6.18),

$$\frac{X_i^0}{\rho g} = \int_{S_B} \phi_D^0 n_i dS = -\int_{S_R} (\phi^I \phi_{i,n}^0 - \phi_i^0 \phi_{,n}^I) dS = \sqrt{\frac{2\pi}{k}} C_g(kh) H_i^0(\beta + \pi) e^{i\pi/4} \quad i = 1, ...6. \tag{65}$$

where $C_g(kh)$ is given by (59) and H_i^0 by (60). We now proceed to derive similar relations for X_i^1. By using the variant of Stokes theorem (55) and the body boundary conditions for ϕ_i^0 and ψ_i^1, see eqs. (25) and (27), we find that X_i^1 may be written

$$\frac{X_i^1}{\rho g} = \int_{S_B} (\phi_D^1 \phi_{i,n}^0 - \phi_D^0 \psi_{i,n}^1) dS = \int_{S_B} (\psi_7^1 \phi_{i,n}^0 - \phi_D^0 \psi_{i,n}^1) dS + \int_{S_B} \phi_7^{11} \phi_{i,n}^0 dS \tag{66}$$

where we have introduced $\psi_7^1 = \phi_7^{12} + \phi_7^{13}$, such that $\phi_D^1 = \phi_7^{11} + \psi_7^1$ (see also Appendix A). Furthermore, $(\ )_{,n}$ denotes $\partial/\partial n$. We may add to (66) the integral $\int_{S_B}(-\phi_i^0\psi_{7,n}^1 + \psi_i^1\phi_{D,n}^0)dS$, which equals zero, since $\psi_{7,n}^1 = \phi_{D,n}^0 = 0$ at S_B. By applying Green's theorem and the body boundary conditions for the involved potentials, the first integral on the right of (66) is converted to integrals over S_F and S_R, i.e.

$$\frac{X_i^1}{\rho g} = -\int_{S_F+S_R}(\psi_7^1\phi_{i,n}^0 - \phi_i^0\psi_{7,n}^1 + \psi_i^1\phi_{D,n}^0 - \phi_D^0\psi_{i,n}^1)dS + \int_{S_B}\phi_7^{11}\phi_{i,n}^0 dS \tag{67}$$

Since $\psi_i^1 = \phi_i^{12} + \phi_i^{13}$, $(i = 1, ...7)$, the integral over S_R in (67) may be written as $I_X^2 + I_X^3$, where

$$I_X^j = -\int_{S_R}(\phi_7^{1j}\phi_{i,n}^0 - \phi_i^0\phi_{7,n}^{1j} + \phi_i^{1j}\phi_{D,n}^0 - \phi_D^0\phi_{i,n}^{1j})dS, \quad j = 2, 3 \tag{68}$$

We may show, by applying the far-field forms of ϕ_i^0 and ϕ_i^{13}, that I_X^3 becomes

$$I_X^3 = \int_{S_R}(\phi^I\phi_{i,n}^{13} - \phi_i^{13}\phi_{,n}^I)dS \tag{69}$$

Next we consider I_X^2. Exploiting that $\phi_7^{12} = 2iK\partial^2\phi_D^0/\partial K\partial\theta$, $\phi_i^{12} = 2iK\partial^2\phi_i^0/\partial K\partial\theta$, and applying partial integration with respect to the θ-variable, we find

$$I_X^2 = -2iK\frac{\partial}{\partial K}\int_{S_R}(\phi_{D,\theta}^0\phi_{i,n}^0 - \phi_i^0\phi_{D,n\theta}^0)dS \tag{70}$$

We may then show, by applying the far-field form of ϕ_i^0, $(i = 1, ...7)$ that the contribution from $\phi_{7,\theta}^0\phi_{i,n}^0 - \phi_i^0\phi_{7,n\theta}^0$ is zero. Then, since $\phi_{,\theta}^I = -\phi_{\beta}^I$,

$$I_X^2 = 2iK\frac{\partial^2}{\partial\beta\partial K}\int_{S_R}(\phi^I\phi_{i,n}^0 - \phi_i^0\phi_{,n}^I)dS \tag{71}$$

Comparing with (65), we find that $I_X^2 = -\int_{S_B}\phi_7^{11}\phi_{i,n}^0 dS$.

Finally, we consider the integral over S_F in (67). By applying the boundary conditions at the free surface for the involved potentials, Green's theorem, the boundary conditions for $\mathbf{w}$ at S_B and S_R, and that S_B is wall-sided at $z = 0$, we find

$$\int_{S_F}(\psi_7^1\phi_{i,n}^0 - \phi_i^0\psi_{7,n}^1 + \psi_i^1\phi_{D,n}^0 - \phi_D^0\psi_{i,n}^1)dS$$
$$= 2iK\int_{S_F}\nabla_h\cdot(\mathbf{w}\phi_i^0\phi_D^0)dS = 2iK\int_{C_B+C_R}\phi_i^0\phi_D^0\mathbf{w}\cdot\mathbf{n}dl = 0 \tag{72}$$

where C_B and C_R denotes the mean water line of S_B and S_R, respectively.

Thus, $X_i^1/\rho g = I_X^3$. By carrying out the integration in (69), applying (32) and the method of stationary phase, we obtain

$$\frac{X_i^1}{\rho g} = -\sqrt{\frac{2\pi}{k}}C_g(kh)H_i^{13}(\beta + \pi)e^{i\pi/4}, \quad i = 1, ...6 \tag{73}$$

Generalized Haskind relations are also derived for a body of general shape moving with a small forward speed (Nossen et al. 1991, Grue and Biberg 1993).

In figure 1 we show the exciting force $iX_{i,\beta}^0 + X_i^1$ in heave and pitch for a ship. The force is obtained by both pressure integration and the generalized Haskind relation, with good agreement between the two different methods. For comparison we also show the corresponding components $|X_i^0|$ of the exciting force, which are much smaller than $|iX_{i,\beta}^0 + X_i^1|$ in these examples. As geometry we choose a ship oriented along the x-axis with section given by a half-circle and beam

$$b(x) = b_0[1 - (2x/l)^4], \quad |x| < l/2, \tag{74}$$

where the length to beam ratio is $l/b_0 = 5.6$, hereafter referred to as Ship 1. The dimensions of Ship 1 correspond to the dimensions of a Turret Production Ship (TPS) (model shown in Grue and Palm 1993, figure 1) which is considered in some examples later. Working with the geometry (74) is advantageous, since refinement of the discretization and thereby convergence tests are easy to perform.

6.2 Added mass and damping

By next setting the wave amplitude equal to zero ($A = 0$) we obtain the components of the force and moment in the radiation problem, i.e.

$$F_i^{rad} = -\rho \int_{S_B} \Big(\frac{\partial \Phi}{\partial t} + \Omega \mathbf{w} \cdot \nabla \Phi\Big) n_i dS \tag{75}$$

Now,

$$-\Big(\frac{\partial \Phi}{\partial t} + \Omega \mathbf{w} \cdot \nabla \Phi\Big) = Re\Big\{\rho\omega^2 e^{i\omega t}\Big[\xi_j^0 \phi_j^0 + \epsilon\Big(\xi_j^1 \phi_j^0 + 2i\frac{\partial \xi_j^0}{\partial \beta}\frac{\partial}{\partial K}(K\phi_j^0) + \xi_j^0(\psi_j^1 - i\mathbf{w}\cdot\nabla\phi_j^0)\Big)\Big]\Big\} \tag{76}$$

Introducing

$$f_{ij}^0 = \rho \int_{S_B} \phi_j^0 n_i dS \tag{77}$$

$$f_{ij}^1 = \rho \int_{S_B} (\psi_j^1 - i\mathbf{w}\cdot\nabla\phi_j^0) n_i dS \tag{78}$$

we find

$$F_i^{rad} = Re\Big\{\omega^2 e^{i\omega t}\Big[\xi_j^0 f_{ij}^0 + \epsilon\Big(\xi_j^1 f_{ij}^0 + 2i\frac{\partial \xi_j^0}{\partial \beta}\frac{\partial}{\partial K}(K f_{ij}^0) + \xi_j^0 f_{ij}^1\Big)\Big]\Big\} \tag{79}$$

f_{ij}^0 and f_{ij}^1 contain the added mass and damping coefficients.

The added mass and damping coefficients obey the well known symmetry relations $f_{ij}^0 = f_{ji}^0$ when $\Omega = 0$. For slender ships with forward speed, the added mass and damping coefficients obey the Timman-Newman symmetry relations. These relations have been generalized for bodies of general shape moving with small forward speed (Wu and Eatock Taylor 1990, Nossen et al. 1991, Grue and Biberg 1993). It is possible to generalize the Timman-Newman relations also to the present case.

We consider the sum $f_{ij}^1 + f_{ji}^1$. By using the variant of Stokes theorem (55), with G^0 replaced by ϕ_j^0, and using the body boundary condition for ψ_j^1, we find

$$f_{ij}^1 + f_{ji}^1 = \rho \int_{S_B} (\psi_j^1 \phi_{i,n}^0 - \phi_i^0 \psi_{j,n}^1 + \psi_i^1 \phi_{j,n}^0 - \phi_j^0 \psi_{i,n}^1) dS \tag{80}$$

This integral may by use of Green's theorem be converted to integrals over S_F and S_R with the same integrand, but multiplied by -1. The integral over S_R becomes

$$-\rho \int_{S_R} (\psi_j^1 \phi_{i,n}^0 - \phi_i^0 \psi_{j,n}^1 + \psi_i^1 \phi_{j,n}^0 - \phi_j^0 \psi_{i,n}^1) dS \tag{81}$$

By using the far-field conditions for ϕ_i^0 and ψ_i^1 (see eq. (31) and eq. (34)), (81) may be written

$$\rho \int_{S_R} \frac{\partial}{\partial \theta}(\phi_i^0 \phi_j^0) dS \tag{82}$$

which equals zero. The integral over S_F, i.e.

$$\rho \int_{S_F} (\psi_j^1 \phi_{i,n}^0 - \phi_i^0 \psi_{j,n}^1 + \psi_i^1 \phi_{j,n}^0 - \phi_j^0 \psi_{i,n}^1) dS \tag{83}$$

becomes zero by using the same argument as in (72). We have then shown that

$$f_{ij}^1 = -f_{ji}^1 \tag{84}$$

Numerical examples of the cross-coupling coefficients between sway and pitch, f_{25}^1, $-f_{52}^1$, and between heave and yaw, f_{36}^1,$-f_{63}^1$, f_{ij}^1, for the two ships illustrate that $f_{ij}^1 \simeq -f_{ji}^1$, in agreement with the theory (figure 2). The results for f_{25}^1, f_{52}^1 are quite similar for the two ships, in spite of their quite different geometries. We note that the cross-coupling coefficients f_{35}^1, f_{53}^1, between heave and pitch become zero for for both ships. (For the symmetric Ship 1 we also have $f_{35}^0 = f_{53}^0$ in all the computations. The zero speed cross-coupling coefficients f_{35}^0, f_{53}^0 are different from zero for the TPS, however.)

6.3 The body responses

Balance of linear and angular momentum for the body gives

$$(F_1, F_2, F_3) - 2\Omega \int_{m_b} \mathbf{k} \times \frac{d\tilde{\mathbf{B}}}{dt} dm = \int_{m_b} \frac{d^2\tilde{\mathbf{B}}}{dt^2} dm \tag{85}$$

$$(F_4, F_5, F_6) - 2\Omega \int_{m_b} \boldsymbol{x} \times (\mathbf{k} \times \frac{d\tilde{\mathbf{B}}}{dt}) dm = \int_{m_b} \boldsymbol{x} \times \frac{d^2\tilde{\mathbf{B}}}{dt^2} dm \tag{86}$$

where the integration is over the body mass (m_b), and where (F_1, F_2, F_3) and (F_4, F_5, F_6) account for the sum of linear pressure forces, gravity and eventual mooring forces. The second term on the left is due to the Coriolis force.

The inertia terms on the right are represented by the usual mass matrix M_{ij} times the motion. By evaluating $d^2\tilde{\mathbf{B}}/dt^2$ we find for the r.h.s. of (85)–(86)

$$-\omega^2 M_{ij} Re[(\xi_j^0 + \epsilon(2i\xi_{j,\beta}^0 + \xi_j^1))e^{i\omega t}] \tag{87}$$

The terms due to the Coriolis force may be represented similarly, i.e.

$$-2i\epsilon\omega^2 M_{ij}^c Re(\xi_j^0 e^{i\omega t}) \tag{88}$$

where the matrix M_{ij}^c is given by

$$M_{ij}^c = \begin{pmatrix} 0 & -m_b & 0 & m_b Z_G & 0 & -m_b X_G \\ m_b & 0 & 0 & 0 & m_b Z_G & -m_b Y_G \\ 0 & 0 & 0 & 0 & 0 & 0 \\ -m_b Z_G & 0 & 0 & 0 & -I_{xy} & D_{yz} \\ 0 & -m_b Z_G & 0 & I_{xy} & 0 & -D_{xz} \\ m_b X_G & m_b Y_G & 0 & -D_{yz} & D_{xz} & 0 \end{pmatrix} \tag{89}$$

Here (X_G, Y_G, Z_G) denotes the centre of gravity, and

$$I_{xy} = \int_{m_b} z^2 dm, \qquad D_{xz} = \int_{m_b} xz dm, \qquad D_{yz} = \int_{m_b} yz dm \tag{90}$$

$I_{x_i x_j}$ and $D_{x_i x_j}$ are the moment of inertia and the centrifugal moment with respect to the $x_i x_j$ plane respectively.

By using (64) for F_i^{ex} and (79) for F_i^{rad}, we find that the equation of motion becomes, to order ϵ^0 and ϵ^1, respectively

$$(-\omega^2(M_{ij} + f_{ij}^0) + c_{ij})\xi_j^0 = AX_i^0 \tag{91}$$

$$(-\omega^2(M_{ij} + f_{ij}^0) + c_{ij})\xi_j^1 = A(X_i^1 + iX_{i,\beta}^0) + \omega^2[(f_{ij}^1 - 2iM_{ij}^c)\xi_j^0 + 2i(M_{ij} + (Kf_{ij}^0)_{,K})\xi_{j,\beta}^0] \tag{92}$$

Here, c_{ij} contains the coefficients of hydrostatic forces plus eventual mooring forces.

6.4 The frequency of oscillation of mode number j

The oscillatory responses of the body read

$$Re(\xi_j e^{i\omega t}) = |\xi_j| Re(e^{i\omega t + i\delta_j}) \tag{93}$$

where the phase angle is determined by $\delta_j = Im \ln \xi_j$, $(\xi_j \neq 0)$. The local frequency of oscillation is then, to first order in ϵ, given by

$$\sigma_j = \omega + \frac{d\delta_j}{dt} = \omega - \Omega \frac{\partial \delta_j^0}{\partial \beta} = \omega - \Omega Im\Big(\frac{1}{\xi_j^0}\frac{\partial \xi_j^0}{\partial \beta}\Big) \qquad (\xi_j^0 \neq 0) \tag{94}$$

Likewise, we may find the frequency of oscillation of, say, the exciting force $Re(X_j e^{i\omega t})$, which becomes

$$\sigma_{X_j} = \omega - \Omega Im\Big(\frac{1}{X_j^0}\frac{\partial X_j^0}{\partial \beta}\Big) \qquad (X_j^0 \neq 0) \tag{95}$$

Examples of the responses in the vertical modes of motion of Ship 1 and the TPS in slow rotation are given in figures 3 – 4. We find that ξ_3^1, ξ_5^1 are much larger than the counterparts at $\Omega = 0$. Furthermore, both figures show that the frequency of the rotating ship becomes different in the heave and pitch modes of motion. For Ship 1 the frequencies of the response and the exciting force are the same in the respective modes, practically speaking, while for the TPS the exciting force X_3 and the response ξ_3 have different frequencies (figure 4c). For this ship, the frequency of X_3 becomes large (but finite) for kl close to 9.2, which is due to that $|X_3^0|$ is very small close to this wave number. Corresponding results apply to the frequencies of ξ_5 and X_5 when kl is close to 13.5.

The properties of the surge motion due to a rotating Ship 1 for wave heading varying between 0° and 180° at a fixed wavenumber is then investigated, for the purpose of further illustration (figure 5). Of interest, among others, is to see how the frequency of oscillation behaves for wave heading close to 90° (beam seas), where the surge motion disappears. The phase δ_1^0 jumps at this wave heading, without, however, affecting the derivative of δ_1^0 with respect to the wave angle, when β tends to 90° from above or below. Even $\partial\delta_1^0/\partial\beta = Im[(\partial\xi_1^0/\partial\beta)/\xi_1^0]$ is smooth and becomes zero for $\beta \rightarrow 90°$, in spite of that $1/\xi_1^0$ becomes infinitely large there.

7 Wave drift damping

The coefficients of the wave drift damping matrix due to a slow angular velocity is then considered. We denote the time-averaged horizontal force by $\overline{\mathbf{F}} = \overline{F}_1\mathbf{i}_1 + \overline{F}_2\mathbf{i}_2$ ($\mathbf{i}_1 = \mathbf{i}, \mathbf{i}_2 = \mathbf{j}$) and the time-averaged moment about the vertical axis by $\overline{M}_6$. The wave drift damping coefficients appear by expanding $\overline{F}_1, \overline{F}_2, \overline{M}_6$ in perturbation series after the angular velocity, i.e.

$$(\overline{F}_1, \overline{F}_2, \overline{M}_6) = (F_{10}, F_{20}, M_{60}) - \epsilon(B_{16}, B_{26}, B_{66}) \tag{96}$$

where F_{10}, F_{20}, M_{60} denote the forces and moment when $\epsilon = 0$ and the last term, proportional to the slow yaw-velocity, is a generalized damping term. The coefficients B_{16}, B_{26}, B_{66} compose the part of the wave drift damping matrix due to the slow angular motion. Following GP for the diffraction problem, we apply conservation of linear and angular momentum to derive formulae for B_{i6}, accounting for terms proportional to the wave amplitude squared times the slow velocity, disregarding higher order terms. The derivations in the coupled radiation-diffraction problem are somewhat more complex than in the diffraction problem, as outlined below, in addition to that the various potentials now contain the complete radiation-diffraction effects.

7.1 The forces B_{16}, B_{26}

Conservation of linear momentum gives

$$\overline{\mathbf{F}} = \epsilon\rho\omega(\mathbf{i}_i\frac{\partial}{\partial\beta} - \mathbf{k}\times\mathbf{i}_i)\overline{\int_V \Phi'_{,x_i}dV} - \mathbf{i}_i\overline{\int_{S_R}(pn_i + \rho\Phi'_{,x_i}\nabla\Phi'\cdot\mathbf{n})dS} \tag{97}$$

where a bar denotes time-average, V the (time-dependent) fluid volume bounded by the vertical circular cylinder S_R, the (moving) free surface and the (moving) body boundary, and sum over $i = 1, 2$ is understood. We consider the last term in (97) first. Following GP we find

$$\begin{aligned} &-\overline{\int_{S_R}(pn_i + \rho\Phi'_{,x_i}\nabla\Phi'\cdot\mathbf{n})dS} \\ &= \frac{\rho g A^2}{4K}\int_{S_R} Re\{\phi(\phi^*_{,x_i})_{,n} - \phi_{,x_i}\phi^*_{,n}\}dS - \epsilon\rho\omega\int_{S_R}(\psi^{(2)}_{,\beta} + \psi^{(2)}_{,\theta})n_i dS \end{aligned} \tag{98}$$

where we have used that $\Phi' = Re\{(iAg/\omega)\phi e^{i\omega t}\} + \Omega\chi_6 + \psi^{(2)}$.

Next we consider evaluation of $\overline{\int_V \Phi'_{,x_i}dV}$. This integral contains some new terms in the complete radiation-diffraction problem due to the body motions, which are not described by the analysis in the diffraction problem. By evaluating the time average we find

$$\overline{\int_V \Phi'_{,x_i}dV} = \int_{S_B}\overline{\Phi_{,x_i}\tilde{\mathbf{B}}\cdot\mathbf{n}}dS + \int_{S_F}\overline{\Phi_{,x_i}\zeta}dS + \int_{\mathcal{V}}\psi^{(2)}_{,x_i}dV \tag{99}$$

where $\tilde{\mathbf{B}}$ is given in (16), ζ denotes the free surface elevation and the integration on the right is over the mean positions of the wetted body surface, the free surface and the fluid volume, S_B, S_F, $\mathcal{V}$, respectively. Since the term $\overline{\int_V \Phi'_{,x_i}dV}$ appears in (97) multiplied by ϵ, it suffices to evaluate (99) to $O(A^2)$. We then find

$$\overline{\int_V \Phi'_{,x_i}dV} = \frac{gA^2}{2\omega}Im\int_{S_B}\mathbf{B}^0\cdot\mathbf{n}\phi^{0*}_{,x_i}dS + \frac{gA^2}{2\omega}Im\int_{S_F}\phi^0\phi^{0*}_{,x_i}dS + \int_{S_B}\psi^{(2)}n_i dS + \int_{S_R}\psi^{(2)}n_i dS \tag{100}$$

where $\mathbf{B}^0$ is given in (45) and we have used the divergence theorem to obtain the two last terms on the right of (100).

The first term on the right of (100) is on final form. The last term multiplied by $\epsilon\rho\omega(\mathbf{i}_i\partial/\partial\beta - \mathbf{k}\times\mathbf{i}_i)$ cancels the last integral of (98). The second term may, by using the divergence theorem, be rewritten

$$Im\int_{S_F}\phi^0\phi^{0*}_{,x_i}dS = Im\int_{S_F}x_i\phi^0\phi^{0*}_{,zz}dS + Im\int_{C_B+C_R}x_i\phi^0\phi^{0*}_{,n}dS \tag{101}$$

To rewrite the third term in (100) we introduce the auxiliary potentials χ_1,χ_2 satisfying $\nabla^2\chi_i$ in the fluid, $\chi_{i,n}=n_i$ at S_B, $\chi_{i,z}=0$ at $z=0,-h$, $|\nabla\chi_i|\to 0$, $(x^2+y^2)^{1/2}\to\infty$. Applying Green's theorem to $\psi^{(2)}$ and χ_i we find

$$\int_{S_B}\psi^{(2)}n_i dS = \int_{S_B+S_F}\chi_i\psi^{(2)}_{,n}dS \tag{102}$$

Inserting the boundary conditions for $\psi^{(2)}$ at $z=0$ and at S_B gives

$$\int_{S_F}\chi_i\psi^{(2)}_{,z}dS = -\frac{A^2g}{2\omega}Im\int_{S_F}\chi_i\phi^0\phi^{0*}_{,zz}dS \tag{103}$$

$$\int_{S_B}\chi_i\psi^{(2)}_{,n}dS = \frac{A^2g}{2\omega}Im\int_{S_F}\chi_i\{\mathbf{B}^0\cdot(\mathbf{n}\cdot\nabla)\nabla\phi^{0*} - \mathbf{C}^0\cdot(K\mathbf{B}^{0*}-\nabla\phi^{0*})\}dS \tag{104}$$

where (44) has been used and $\mathbf{C}^0$ is defined in (45).

The integral over $\chi_i\mathbf{B}^0\cdot(\mathbf{n}\cdot\nabla)\nabla\phi^{0*}$ in (104) may be simplified. By using a variant of Stokes' theorem (GP, eq. B3) we find

$$\int_{S_B}\chi_i\mathbf{B}^0\cdot(\mathbf{n}\cdot\nabla)\nabla\phi^{0*}dS = \int_{S_B}\{\mathbf{n}\cdot(\nabla\phi^{0*}\cdot\nabla)(\chi_i\mathbf{B}^0) + K\mathbf{B}^0\cdot\mathbf{n}\nabla\cdot(\chi_i\mathbf{B}^{0*})\}dS - \int_{C_B}\chi_i K\mathbf{B}^0\cdot\mathbf{n}(\phi^{0*}+B_3^{0*})dl \tag{105}$$

where $B_3^0=\mathbf{k}\cdot\mathbf{B}^0$. By then using that $\nabla\cdot\mathbf{B}^0=0$ and that

$$\mathbf{n}\cdot(\nabla\phi^{0*}\cdot\nabla)(\chi_i\mathbf{B}^0) = \mathbf{B}^0\cdot\mathbf{n}\nabla\chi_i\cdot\nabla\phi^{0*} - \chi_i\mathbf{C}^0\cdot\nabla\phi^{0*} \tag{106}$$

we find

$$\int_{S_B}\chi_i\psi^{(2)}_{,n}dS = \frac{A^2g}{2\omega}Im\Big(-\int_{S_B}\mathbf{B}^0\cdot\mathbf{n}\nabla\chi_i\cdot\nabla\phi^{0*}dS + \int_{C_B}K\mathbf{B}^0\cdot\mathbf{n}\chi_i\phi^{0*}dl\Big) + I \tag{107}$$

where

$$I = \frac{\omega A^2}{2}Im\Big(\int_{C_B}\mathbf{B}^0\cdot\mathbf{n}B_3^{0*}\chi_i dl - \int_{S_B}\mathbf{B}^0\cdot\mathbf{n}\mathbf{B}^{0*}\cdot\nabla\chi_i dS + \int_{S_B}\mathbf{B}^{0*}\cdot\mathbf{C}^0\chi_i dS\Big) \tag{108}$$

We may show that $I=0$. From the first and second term of (108) we find

$$\begin{aligned}&\int_{C_B}\mathbf{B}^0\cdot\mathbf{n}B_3^{0*}\chi_i dl - \int_{S_B}\mathbf{B}^0\cdot\mathbf{n}\mathbf{B}^{0*}\cdot\nabla\chi_i dS\\ &= \frac{1}{2}\int_{C_B}(\mathbf{B}^0\times\mathbf{B}^{0*})\cdot(\mathbf{n}\times\mathbf{k})\chi_i dl - \frac{1}{2}\int_{S_B}(\mathbf{B}^0\times\mathbf{B}^{0*})\cdot(\mathbf{n}\times\nabla\chi_i)dS\\ &= \frac{1}{2}\int_{S_B}\chi_i\nabla\times(\mathbf{B}^0\times\mathbf{B}^{0*})dS\end{aligned} \tag{109}$$

where we have used Stokes' theorem in the last step. By then expanding the integrand on the right we find that (109) is equal to $-\int_{S_B} \mathbf{B}^{0*}\cdot\mathbf{C}^0\chi_i dS$, which gives that $I=0$.

We then introduce $\phi=\phi^0+\epsilon\phi^1$ into (98) and insert (98), (100)-(107) into (96)–(97), finding

$$\frac{B_{16}\mathbf{i}+B_{26}\mathbf{j}}{\rho g A^2} = -(\mathbf{i}_i\frac{\partial}{\partial\beta}-\mathbf{k}\times\mathbf{i}_i)M_i-(\mathbf{i}_i\frac{\partial}{\partial\beta}-\mathbf{k}\times\mathbf{i}_i)\frac{1}{2}Im\int_{C_R}x_i\phi^0\phi^{0*}_{,n}dl$$
$$-\frac{1}{4K}\int_{S_R}Re\{\phi^0(\nabla_h\phi^{1*})_{,n}+\phi^1(\nabla_h\phi^{0*})_{,n}-\phi^0_{,n}\nabla_h\phi^{1*}-\phi^1_{,n}\nabla_h\phi^{0*}\}dS \tag{110}$$

where

$$M_i=\frac{1}{2}Im\Big(-\int_{S_B}\mathbf{B}^0\cdot\mathbf{n}(\nabla\chi_i-\mathbf{i}_i)\cdot\nabla\phi^{0*}dS+K\int_{C_B}(\chi_i-x_i)\mathbf{B}^0\cdot\mathbf{n}\phi^{0*}dl-\int_{S_F}(\chi_i-x_i)\phi^0\phi^{0*}_{,zz}dS\Big) \tag{111}$$

We show in §7.3 that M_i $(i=1,2)$ correspond to the far-field dipole moments of $\psi^{(2)}$. The two latter integrals of (110) may be developed along the lines of GP, who considered the infinite depth case. The analysis, here generalized to an arbitrary water depth, gives after some algebra

$$\frac{B_{16}\mathbf{i}+B_{26}\mathbf{j}}{\rho g A^2} = -(\mathbf{i}_i\frac{\partial}{\partial\beta}-\mathbf{k}\times\mathbf{i}_i)M_i$$
$$+\frac{1}{2}\int_0^{2\pi}Re\Big\{H^0(\theta)H^{1*}(\theta)\begin{pmatrix}\cos\theta\\ \sin\theta\end{pmatrix}-2iH^0(\theta)\Big[H^0_{,\beta\theta}(\theta)+H^0_{,\theta\theta}(\theta)\Big]^*\begin{pmatrix}-\sin\theta\\ \cos\theta\end{pmatrix}\Big\}d\theta$$
$$+\frac{1}{2}Re\Big\{\sqrt{\frac{2\pi}{k}}e^{i\pi/4}\Big[H^{1*}(\beta)\begin{pmatrix}\cos\beta\\ \sin\beta\end{pmatrix}-2i\Big[H^0_{,\beta\theta}(\beta)+H^0_{,\theta\theta}(\beta)\Big]^*\begin{pmatrix}-\sin\beta\\ \cos\beta\end{pmatrix}\Big]\Big\} \tag{112}$$

where the amplitude function H^1 is given by

$$H^1=\frac{kC_g}{K}(2iK(H^0_{,\beta K}+H^0_{,\theta K})+H^{13})+\frac{ik}{C_g}\frac{\partial C_g}{\partial k}(H^0_{,\beta}+H^0_{,\theta}) \tag{113}$$

and H^{13} is defined in (42). This means that B_{16} and B_{26} are expressed by the far-field dipole moments $(\tilde{M}_1, M_2)$ of $\psi^{(2)}$ and the far-field amplitudes of the linear potentials. These formulae are valid for arbitrary constant water depth and arbitrary linear body responses, and generalize the formulae of Newman (1993) and GP, which were derived for the diffraction problem at infinite water depth.

7.2 The moment B_{66}

Conservation of angular momentum gives for the moment $\overline{M}_6$

$$\overline{M}_6=\epsilon\rho\omega\frac{\partial}{\partial\beta}\overline{\int_V\mathbf{k}\cdot(\boldsymbol{x}\times\nabla\Phi')dV}+\rho\overline{\int_{S_R}\mathbf{k}\cdot(\boldsymbol{x}\times\nabla\Phi'\nabla\Phi'\cdot\mathbf{n})dS} \tag{114}$$

The latter term on the right of (114) becomes

$$-\frac{\rho g A^2}{2K}\Big[\int_{S_R}Re\{\phi^0_{,\theta}\phi^{0*}_{,n}\}dS+\epsilon\int_{S_R}Re\{\phi^0_{,\theta}\phi^{1*}_{,n}+\phi^1_{,\theta}\phi^{0*}_{,n}\}dS\Big] \tag{115}$$

where we have inserted $\Phi' = \Phi = Re\{(iAg/\omega)(\phi^0 + \epsilon\phi^1)\}$, taken a time-average and kept the leading terms. We next consider the first term on the right of (114). By evaluating the time-average and using the divergence theorem we find (to leading order)

$$\overline{\int_V \mathbf{k}\cdot(\boldsymbol{x}\times\nabla\Phi')dV} = \frac{gA^2}{\omega} Im\Big(\int_{S_B} \mathbf{B}^0\cdot\mathbf{n}\phi^{0*}_{,\theta}dS + \int_{S_F} \phi^0\phi^{0*}_{,\theta}dS\Big) + \int_{S_B} \psi^{(2)}n_6 dS \qquad (116)$$

The last term on the right of (116) may be rewritten similarly as (102)-(107) (with $I = 0$ in (107)), giving

$$\int_{S_B} \psi^{(2)}n_6 dS = -\frac{gA^2}{2\omega} Im\Big(\int_{S_F} \chi_6\phi^0\phi^{0*}_{,zz}dS + \int_{S_B} \mathbf{B}^0\cdot\mathbf{n}\nabla\chi_6\cdot\nabla\phi^{0*}dS - K\int_{C_B} \mathbf{B}^0\cdot\mathbf{n}\chi_6\phi^{0*}dl\Big) \qquad (117)$$

Inserting (114)-(117) into (96) we find for B_{66}

$$\begin{aligned}\frac{B_{66}}{\rho g A^2} &= \frac{1}{2}\frac{\partial}{\partial\beta}\int_{S_B} Im\{\mathbf{B}^0\cdot\mathbf{n}\mathbf{w}\cdot\nabla\phi^{0*}\}dS - \frac{K}{2}\frac{\partial}{\partial\beta}\int_{C_B} Im\{\mathbf{B}^0\cdot\mathbf{n}\chi_6\phi^{0*}\}dl \\ &+\frac{1}{2}\frac{\partial}{\partial\beta}\int_{S_F} Im\{\chi_6\phi^0\phi^{0*}_{,zz} + \phi^0_{,\theta}\phi^{0*}\}dS + \frac{1}{2K}\int_{S_R} Re\{\phi^0_{,\theta}\phi^{1*}_{,n} + \phi^1_{,\theta}\phi^{0*}_{,n}\}dS \qquad (118)\end{aligned}$$

The sum of the second and third integral in (118) may be rewritten. By exploiting the boundary conditions for ϕ^0, ϕ^1 and χ_6 at S_B and S_F, and applying the divergence theorem twice we may show that this sum becomes

$$-\frac{1}{2K}\int_{S_F} Re\{\phi^{0*}_{,\beta}\phi^1_{,n} - \phi^1\phi^{0*}_{,\beta n}\}dS \qquad (119)$$

By applying Green's theorem to $\phi^0_{,\beta}$ and ϕ^1, (119) may be recast into integrals over S_B and S_R, giving for B_{66}

$$\begin{aligned}\frac{B_{66}}{\rho g A^2} &= \frac{1}{2K}\int_{S_B} Re\{\phi^{0*}_{,\beta}\phi^1_{,n} - \phi^1\phi^{0*}_{,\beta n} - \frac{\partial}{\partial\beta}(iK\mathbf{B}^0\cdot\mathbf{n}\mathbf{w}\cdot\nabla\phi^{0*})\}dS \\ &\frac{1}{2K}\int_{S_R} Re\{(\phi^{0*}_{,\beta} + \phi^{0*}_{,\theta})\phi^1_{,n} - \phi^{1*}(\phi^0_{,\beta} + \phi^0_{,\theta})_{,n}\}dS \qquad (120)\end{aligned}$$

The first integral in (120) may be further developed by exploiting the body boundary conditions for ϕ^0 and ϕ^1, and by using the equations of motion (91)-(92), i.e.

$$\begin{aligned}&\frac{1}{2K}\int_{S_B} Re\{\phi^{0*}_{,\beta}\phi^1_{,n} - \phi^1\phi^{0*}_{,\beta n} - \frac{\partial}{\partial\beta}(iK\mathbf{B}^0\cdot\mathbf{n}\mathbf{w}\cdot\nabla\phi^{0*})\}dS \\ &= -\frac{1}{2}Re\{\xi^{0*}_{i,\beta}(\frac{i}{K}X^0_{i,\beta} + X^1_i + Kf^0_{ij}\xi^1_j + Kf^1_{ij}\xi^0_j + 2i(Kf^0_{ij})_{,K}\xi^0_{j,\beta}) - \xi^{1*}_i(X^0_i + Kf^0_{ij}\xi^0_j)_{,\beta}\} \\ &= Im\Big(\frac{K}{\rho A^2}M^c_{ij}\xi^{0*}_{i,\beta}\xi^0_j + \frac{ic_{ij}}{2\rho g A^2}(\xi^{0*}_{i,\beta}\xi^1_j - \xi^{1*}_i\xi^0_{,\beta})\Big) \qquad (121)\end{aligned}$$

By introducing the far-field form of the potentials ϕ^0 and ϕ^1 into the last term of (120) and evaluating the integrals we finally arrive at

$$\frac{B_{66}}{\rho g A^2} = Im\Big\{\frac{K}{\rho A^2}M^c_{ij}\xi^{0*}_{i,\beta}\xi^0_j + \frac{ic_{ij}}{2\rho g A^2}(\xi^{0*}_{i,\beta}\xi^1_j - \xi^{1*}_i\xi^0_{j,\beta}) - \frac{1}{2k}\int_0^{2\pi}(H^0_{,\beta}(\theta) + H^0_{,\theta}(\theta))H^{1*}(\theta)d\theta\Big\} \qquad (122)$$

The formula for B_{66} contains in the coupled radiation-diffraction problem two extra terms which are completely absent in the diffraction problem. The first term is expressed by the linear body responses and the matrix (89) representing the Coriolis force in the equation governing the linear motions. The second term is expressed by the hydrostatic coefficients c_{ij}, and becomes zero for symmetric restoring force matrix c_{ij}, which usually is the case (moorings may introduce a non-symmertric c_{ij}). The formula for the wave drift damping moment is valid for arbitrary water depth and arbitrary linear body motions. For the diffraction problem, the formulae for B_{66} by Newman (1993), GP and Grue (1996) are recovered.

7.3 Comments on the formulae for B_{i6} and numerical examples

The final formulae for the wave drift damping coefficients are expressed by the far-field amplitudes of the linear potentials and by the linear potentials and response amplitudes of the floating body. In order to interpret the integrals over S_B and S_F in (112) more closely we consider the potential $\psi^{(2)}$ for $R = (x^2 + y^2)^{-1/2} \to \infty$.

Let $g^0(\boldsymbol{x}', \boldsymbol{x})$ denote the Green function G^0 in the limit $K \to 0$. Then g^0 satisfies the rigid wall condition at $z = 0, -h$, and $|\nabla g^0| \to 0$ for $R \to \infty$. Green's theorem applied to $\psi^{(2)}$ and g^0 gives

$$4\pi\psi^{(2)}(\boldsymbol{x}) = \int_{S_B+S_F} g^0 \psi^{(2)}_{,n} dS - \int_{S_B+S_F} g^0_{,n} \psi^{(2)} dS, \qquad \boldsymbol{x} \in \mathcal{V} \tag{123}$$

Following Grue and Palm (1993) for the infinite depth case, we find for $R \to \infty$

$$4\pi\psi^{(2)}(\boldsymbol{x}) = (A^2 g/\omega)\Big(Q g^0(0, \boldsymbol{x}) + (\tilde{M}_1, \tilde{M}_2) \cdot \nabla g^0(0, \boldsymbol{x}) + ...\Big) \tag{124}$$

where

$$g^0(0, \boldsymbol{x}) = (R^2 + z^2)^{-1/2} + \sum_{n=1}^{\infty} \Big((R^2 + (2nh - z)^2)^{-1/2} + (R^2 + (2nh - z)^2)^{-1/2} - \frac{1}{nh} \Big) \tag{125}$$

$$(A^2 g/\omega) Q = \int_{S_B} g^0 \psi^{(2)}_{,n} dS \tag{126}$$

$$(A^2 g/\omega) M_i = \int_{S_B} \psi^{(2)} n_i dS - \int_{S_B+S_F} x_i \psi^{(2)}_{,n} dS \tag{127}$$

Using (102) we find that $(A^2 g/\omega)\tilde{M}_i = \int_{S_B+S_F} (\chi_i - x_i)\psi^{(2)}_{,n} dS$. By then applying (107) with χ_i replaced by $\chi_i - x_i$, and inserting the boundary condition for $\psi^{(2)}_{,n}$ at $z = 0$, we find that $\tilde{M}_i = M_i$.

Computations of the wave drift damping coefficients B_{i6} are performed for the two ship models described in section 6.1, see figures 6-8. The wave angles are 90° (beam seas), 135° (quartering seas), 157°, 180° (head seas) and the wavenumber is in the range $4 < kl < 16$. For a ship with length $l = 230m$ the corresponding wave length λ is in the interval $90m < \lambda < 360m$. The computations show that B_{i6} not only depend on the length to beam ratio of a ship, but also on the detailed form of the ship geometry. This is an expected result, among others since the two geometries have different motion characteristics, see §6.4, with corresponding different contributions in the final formulae for the wave drift damping coefficients and wave drift force and moment. The results for the two ships may differ quite significantly for wave headings in the range between beam seas (90°) and quartering seas (135°), depending on the wavenumber. However, there are also some differences for wave headings close to 180°.

We may compare computations of B_{i6} with and without radiation effects, where results for the latter were given in GP. Such a comparison shows that B_{i6}, with the complete radiation-diffraction effects included, are pronounced for moderate wave lengths, and may have quite large peaks or rapid variations close to the resonances in the vertical modes of motion. For longer waves ($kl < 5$) B_{i6} are small. The results in the diffraction problem exhibit more monotonous behaviour of B_{i6} than in the complete radiation-diffraction problem.

The computations exhibit a positive damping moment B_{66} for the two ship models. The damping also becomes larger for the TPS than for Ship 1, which is most pronounced in beam seas. The generalized damping forces B_{16} and B_{26} may become both positive and negative. It appears to be no physical reasons which contradict the latter results. The wave drift damping computations are also compared with the forces and moment for $\epsilon = 0$, which are displayed in figure 9 for the TPS. We observe that the magnitude of B_{i6} is much larger than (F_{10}, F_{20}, M_{60}). We have, for example, that $B_{66}/M_{60} \simeq 300$ at the peak for $kl \simeq 10$ and $\beta = 90°$. Thus, even for very small $\epsilon = \Omega/\omega$ the effect of a rotation on the total moment may be rather large. A similar result applies to the longitudinal force $\overline{F}_1$. The effect of a rotation is somewhat smaller for the lateral force $\overline{F}_2$.

8 Discussion of various aspects of the method

8.1 Convergence and energy balance

Convergence properties of the induced forces computed by the employed low-order method are discussed by Newman and Lee (1992) in the case when there is no slow motion. Convergence of the present method is here illustrated for some of the global quantities. The added mass and damping coefficients, f^1_{ij} and $-f^1_{ji}$, should be equal, according to the theory. Computations for Ship 1 of f^1_{25} and $-f^1_{52}$ versus the inverse number of panels ($1/N_B$) on the wetted surface are shown in figure 10, indicating that $f^1_{25} + f^1_{52} \to 0$ as $1/N_B \to 0$. The results indicate a relative error of about 1% in $|f^1_{52}|$ and $|f^1_{25}|$, for the finest discretization. The phase of the force has a somewhat poorer accuracy, on the other hand. Computations of the wave drift damping coefficients B_{16} and B_{66} with various discretizations of Ship 1 are next illustrated and document convergence, see figure 11. The results further show that quite good estimates of the wave drift damping coefficients may be obtained by even a rather coarse discretization of the geometry.

It is also of interest to invoke the energy equation for the floating body. This becomes

$$\frac{dE_b}{dt} = \int_{S_B} p\mathbf{v} \cdot \mathbf{n} dS \tag{128}$$

($\mathbf{n}$ points into the body) expressing that the work due to the pressure force acting on the body per unit time is equal to the rate of change of kinetic plus potential energy of the body (E_b). The energy equation gives, alternatively,

$$\frac{d(E_b + E_f)}{dt} = -\int_{S_R} (p + \frac{1}{2}\rho\mathbf{v}^2 + \rho g z)\mathbf{v} \cdot \mathbf{n} dS \tag{129}$$

($\mathbf{n}$ points outwards) expressing that the rate of change of kinetic plus potential energy of the floating body and the fluid ($E_b + E_f$) inside the control surface S_R is equal to the energy flux at S_R. Let us consider the time-averaged energy equation. The difference

$$W = -\overline{\int_{S_R} (p + \frac{1}{2}\rho \mathbf{v}^2 + \rho g z)\mathbf{v} \cdot \mathbf{n} dS} - \overline{\frac{d(E_b + E_f)}{dt}} \tag{130}$$

should then be equal to zero in the numerical model. Expanding W by $W = W^0 + \epsilon W^1 + ...$, we develop formulae for W^0 and W^1 in Appendix C. The quantity W^1 is expressed by an integral over the wetted body surface, terms due to the time-averaged second order motion of the floating body, expressing the rate of change of the potential energy of the body and the fluid with respect to the wave angle, and finally a contribution involving far-field amplitudes of the potentials. We have investigated the energy balance for several geometries and find that it is satisfied to a good accuracy in all cases; an example is shown in figure 12.

8.2 Comparison with the translational case

By letting the body rotate about an axis at a large distance s, the slow motion becomes effectively unidirectional. In this case we expect to recover the results due to a slow translatory velocity of the body. In an example Ship 1 is rotating about an axis located at $x = 0$, $y = s = 100l$ away from the ship. We compare computations in head waves of B_{16}/sK obtained by (112) and B_{66}/s^2K obtained by (122), which shall coincide with this scaling, approximately. (The only difference should be due to the very slow rotation about the vertical axis of the ship.) We also compare with the wave drift damping coefficient B_{11}, i.e. the x-component of the wave drift damping force due to slow speed in the x-direction. The latter is obtained by the method of Nossen et al. (1991, eq. 68). The results show that the three completely different formulae give the same scaled wave drift damping coefficient, approximately, in this example, see figure 13.

Recently, Aranha (1996) has studied wave effects on a floating body with slow unidirectional speed in deep water, and has proposed simplified formulae for the far-field amplitude H^U of the linear outgoing wave, his formula (18a), and for the mean drift force, and thereby the wave drift damping coefficient B_{11}, his formula (4). It is of interest to compare results using his and our formulae for the translatory problem, which may be recovered by the present formulation (see also Nossen et al. 1991). First we consider examples of the linear far-field amplitude, H^U. Our and his formulae agree for zero speed, thus we subtract the zero speed value, i.e.

$$H^U - H^0 \equiv \frac{U\omega}{g} H^{1U} \tag{131}$$

and neglect terms proportional to $O(U^2)$. As geometries Ship 1 and a hemisphere are applied, which both may respond freely to the waves. The computations show, however, generally bad agreement between our method and his proposed formula for H^U, for both geometries, see figures 14 and 15b. (There is close agreement for $\theta = 0$, i.e. the polar angle in the opposite direction of the incoming waves ($\beta = \pi$).) Next we consider predictions of the wave drift damping coefficient B_{11}. In the case of the ship there is bad agreement for non-dimensional wavenumber larger than about 6, see figure 13. We have also performed computations for other geometries (ships) and find in general bad agreement between our and his formulae. This conclusion is also true for a restrained ship (the diffraction problem). However, as noted by Aranha, his formula give a quite good prediction of B_{11} for a floating hemisphere, see figure 15a (our recomputation). This is also true for an array of restrained vertical circular cylinders, as first noted by Clark, Malenica and Molin (1993).

9 Conclusion

We have considered the complete radiation-diffraction problem due to a floating body performing a rotation about the vertical axis in incoming waves. The rotation angle may be an arbitrary slowly varying function of time. The mathematical problem is formulated in a relative frame of reference following the slow rotation of the body, accounting for non-Newtonian forces (the Coriolis force). First, the radiation problem coupled to the slow yaw motion of the body is formulated. Thereafter is shown how the various components of the velocity potential may be obtained as solution of integral equations. The mathematical problem is formulated consistently to second order in the wave amplitude and to first order in the slow angular velocity of the body. Therefore, we need to account for steady second order velocities in the fluid which are forced by inhomogeneous boundary conditions at the mean position of the free surface and the body surface.

The linear forces and motions induced by incoming waves are next considered. The exciting forces are obtained by both pressure integration and generalized Haskind relations, accounting for the slow rotation of the body. The added mass and damping obey generalized Timman-Newman relations. Both the latter and the generalized Haskind relations are deduced from precise mathematical arguments, and are valid for geometries of arbitrary shape being wall-sided at the waterline. The linear body responses are obtained from the equation of motion, and we find that their frequencies of oscillation may in general be different. Even the frequency of the exciting force and the response in the same mode may differ in general.

The ultimate goal of the paper has been to give a complementary contribution to a method for obtaining the complete wave drift damping matrix for bodies of general shape, based on a panel method. We derive explicit formulae for the wave drift damping coefficients in the yaw mode of motion, see (112) and (122). These formulae are easy to evaluate once the various components of the velocity potential are determined. The wave drift damping coefficients are expressed by the far-field amplitudes of the linear radiation-diffraction potentials, the far-field dipole moment of the velocity potential $\psi^{(2)}$, and, for B_{66}, a contribution due to linear body responses coupled by the matrix (89) representing the effect of the Coriolis force.

The method is implemented in a computer code suitable for computations on e.g. a work station. Numerical examples are obtained for the global quantities due to two different ships. We have found that relatively accurate predictions may be achieved by applying about 800 quadrilaterals on the ship surface and about 3000 on the free surface, discretized out to an outer circle with a radius of one ship length. Computations of the wave drift damping coefficients are performed for various wave headings and wavenumbers. We find always a positive damping moment B_{66} for the two ship models. We note, however, that B_{66} may in some cases become negative for arrays of vertical cylinders, see Grue (1996). The computations show that the damping forces B_{16} and B_{26} may become both positive and negative. We have invoked the energy balance in the model, finding that this is satisfied to a good accuracy.

When the rotation axis is moved far away from the body, the slow motion becomes effectively unidirectional, and results of the translational case are recovered. In this connection we compare with formulae proposed by Aranha (1996), however, with generally bad agreement, both for the coupled radiation-diffraction problem and for the pure diffraction problem, see §8.2 for more details. However, Aranha's formula for the wave drift damping coefficient in the surge mode of motion gives a quite good prediction for a floating hemisphere and for an array of fixed vertical circular cylinders.

This work was conducted under the Joint Industry Project 'The complete wave drift damping matrix and applications'. We gratefully acknowledge the financial support from Det Norske Veritas, Mobil, Norsk Hydro and Statoil. The WAMIT radiation-diffraction program was provided by Massachusetts Institute of Technology and Det Norske Veritas.

A The potentials in the diffraction problem

We shortly describe the potentials in diffraction problem, outlined by GP, for completeness. The potential ϕ_D is expanded by

$$\phi_D = \phi_D^0 + \epsilon\phi_D^1, \quad \phi_D^0 = \phi^I + \phi_7^0, \quad \phi_D^1 = \phi_7^{11} + \phi_7^{12} + \phi_7^{13} \tag{132}$$

Here, ϕ_D^0 satisfies $-K\phi_D^0 + \partial\phi_D^0/\partial z = 0$ at the free surface and $\partial\phi_D^0/\partial n = 0$ at the body boundary. Furthermore, ϕ_7^{11} and ϕ_7^{12} satisfy

$$-K\phi_7^{11} + \frac{\partial\phi_7^{11}}{\partial z} = 2iK\frac{\partial\phi_D^0}{\partial\beta} \quad \text{at} \quad z = 0 \tag{133}$$

$$\frac{\partial\phi_7^{11}}{\partial n} = 0 \quad \text{at} \quad S_B \tag{134}$$

$$-K\phi_7^{12} + \frac{\partial\phi_7^{12}}{\partial z} = 2iK\frac{\partial\phi_D^0}{\partial\theta} \quad \text{at} \quad z = 0 \tag{135}$$

$$-K\phi_7^{13} + \frac{\partial\phi_7^{13}}{\partial z} = -2iK\nabla_h\phi_D^0\cdot\nabla_h\chi_6 - iK\phi_D^0\nabla_h^2\chi_6 \quad \text{at} \quad z = 0 \tag{136}$$

$$\frac{\partial\phi_7^{12}}{\partial n} + \frac{\partial\phi_7^{13}}{\partial n} = 0 \quad \text{at} \quad S_B \tag{137}$$

The potentials ϕ_7^{11} and ϕ_7^{12} may be expressed by ϕ_D^0 by

$$\phi_7^{11} = 2iK\frac{\partial^2\phi_D^0}{\partial K\partial\beta}, \quad \phi_7^{12} = 2iK\frac{\partial^2\phi_D^0}{\partial K\partial\theta} \tag{138}$$

The far-field amplitudes of ϕ_7^0 and ϕ_7^{13} are given by GP eqs. (4.19) and (4.21), respectively,

$$4\pi H_7^0 = -\int_{S_B}\phi_7^0 h_{,n}^0 dS \tag{139}$$

$$4\pi H_7^{13} = -\int_{S_B}(\psi_7^1 h_{,n}^0 dS - 2iK\phi_{7,K}^0 h_{,\theta n}^0)dS + \int_{S_F}\phi_7^0 L_h(h^0,\chi_6)dS \tag{140}$$

where in the finite depth case h^0 given by (41).

B Remarks on the numerical implementation

The set of integral equations are solved by means of a low-order panel method (an extension of WAMIT). The body surface and the free surface are discretized by quadrilaterals (panels), and the potential or source strength is taken as constant at each panel. The Green function G^0 and its derivatives (G^1) involved in the integral equations have singularities $\nabla(1/r)$, $\nabla(1/r_1)$, $1/r$, $1/r_1$, where $r = |\boldsymbol{x} - \boldsymbol{x}'|$ and $r_1 = [(x-x')^2 + (y-y')^2 + (z+z')^2]^{1/2}$. The singularities are integrated separately over each panel by analytical methods. Numerical integration is otherwise performed using the midpoint rule.

C Conservation of energy

From (130) we have

$$W = -\overline{\int_{S_R} (p + \frac{1}{2}\rho \mathbf{v}^2 + \rho g z)\mathbf{v}\cdot\mathbf{n} dS} - \overline{\frac{d(E_b + E_f)}{dt}} \quad (141)$$

Now,

$$-\overline{\int_{S_R} (p + \frac{\rho}{2}\mathbf{v}^2 + \rho g z)\mathbf{v}\cdot\mathbf{n} dS} = \frac{\rho g^2 A^2}{2\omega}\int_{S_R} Re\{(i\phi - \epsilon\phi_{,\beta})\phi^*_{,n}\} dS \quad (142)$$

Using that $\overline{d(E_b + E_f)/dt} = -\Omega\overline{\partial/(E_b + E_f)/\partial\beta}$, we may show

$$-\overline{\frac{d}{dt}}E_b = \epsilon\omega\frac{\partial}{\partial\beta}\Big[\frac{1}{4}\omega^2\xi_i^0\xi_j^{0*}M_{ij} - \frac{1}{4}m_b g(|\xi_4^0|^2 + |\xi_5^0|^2)Z_G + \frac{1}{2}m_b g Re\{\xi_6^0(\xi_4^{0*}X_G + \xi_5^{0*}Y_G)\}\Big] \quad (143)$$

where (X_G, Y_G, Z_G) denotes the centre of gravity of the body. Furthermore,

$$-\overline{\frac{d}{dt}}E_f = \epsilon\frac{\partial}{\partial\beta}\Big[\frac{\rho g^2 A^2}{4\omega}\Big(\int_{S_B} Re\{K\mathbf{B}^0\cdot\mathbf{n}\phi^{0*}\}dS + 2\int_{S_F} K|\phi^0|^2 dS + \int_{S_R} Re\{\phi^0\phi^{0*}_{,n}\}dS\Big)$$
$$+\frac{\rho g\omega}{4}\Big(\int_{S_B}|B_3^0|^2 n_3 dS + (|\xi_4^0|^2 + |\xi_5^0|^2)Z_B V_B - Re\{2\xi_6^0(\xi_4^{0*}X_B + \xi_5^{0*}Y_B)V_B\}\Big)\Big] \quad (144)$$

where (X_B, Y_B, Z_B) denotes the centre of bouyancy of the body and V_B the displaced volume. Expanding $W = W^0 + \epsilon W^1$ we find

$$\frac{W^0}{\rho g A^2 c_g} = -\frac{1}{C_g} Im\int_{S_R}\phi^0\phi^{0*}_{,n} dS \quad (145)$$

$$\frac{W^1}{\rho g A^2 c_g} = \frac{1}{C_g}\Big\{-\frac{K}{\rho A^2}\frac{\partial}{\partial\beta}Re\{\xi_6^0(\xi_4^{0*}(\rho V_B X_B - m_b X_G) + \xi_5^{0*}(\rho V_B Y_B - m_b Y_G))\}$$
$$+\frac{K}{2\rho A^2}\frac{\partial}{\partial\beta}(|\xi_4^0|^2 + |\xi_5^0|^2)(\rho V_B Z_B - m_b Z_G) + \frac{K^2}{2\rho A^2}\frac{\partial}{\partial\beta}(\xi_i^0\xi_j^{0*})M_{ij}$$
$$+\int_{S_B} Re\{K\mathbf{B}^0\cdot\mathbf{n}(\phi^0_{,\beta} - i(\phi_7^{11} + K(\xi^0_{j,\beta}/A)\phi_j^{11}))^*\}dS + \frac{1}{2}\frac{\partial}{\partial\beta}\int_{S_B} K|B_3^0/A|^2 n_3 dS$$
$$-\int_0^{2\pi} Re\Big[KH^0\Big(\frac{C_g}{K}\tilde{H}^1 + \frac{i}{C_g}\frac{\partial C_g}{\partial k}H^0_{,\theta} - 2iC_g(H^0_{7,K\beta} + K(\xi^0_{j,\beta}/A)H^0_{j,K})\Big)^*\Big]d\theta$$
$$-Re\Big[\sqrt{\frac{2\pi}{k}}e^{i\pi/4}K\Big(\frac{C_g}{K}\tilde{H}^1 + \frac{i}{C_g}\frac{\partial C_g}{\partial k}H^0_{,\theta} - 2iC_g(H^0_{7,K\beta} + K(\xi^0_{j,\beta}/A)H^0_{j,K})\Big)^*\Big]$$
$$+K(\frac{1}{k} + \frac{1}{C_g}\frac{\partial C_g}{\partial k})Re\{i\sqrt{\frac{2\pi}{k}}e^{i\pi/4}H^{0*}_{,\theta}\}\Big\} \quad (146)$$

where

$$\tilde{H}^1 = 2iK(H^0_{,\beta K} + H^0_{,\theta K}) + H^{13} \quad (147)$$

For a floating body we have $\rho V_B = m_b$, $X_B = X_G$, $Y_B = Y_G$. Then the second term in the parenthesis on the right of (146) vanishes.

References

[1] Aranha, J. A. P., Second-order horizontal steady forces and moment on a floating body with small forward speed. *J. Fluid Mech.* **313**, pp. 39-54, 1996.

[2] Clark, P. J., Malenica, S. and Molin, B., An heuristic approach to wave drift damping. *Appl. Ocean Res.* **15**, 1993, 53-55.

[3] Emmerhoff, O. J. and Sclavounos, P. D., The slow-drift motion of arrays of vertical cylinders. *J. Fluid Mech.* **242**, 1992, 31-50.

[4] Emmerhoff, O. J. and Sclavounos, P. D., The simulation of slow-drift motions of offshore structures. *Appl. Ocean Res.* **18**, 1996, 55-64.

[5] Grue, J., Interaction between waves and slowly rotating floating bodies. In: Grue, J., Gjevik, B. and Weber, J. E. *Waves and nonlinear processes in hydrodynamics.* Festschrift for Professor Enok Palm on his seventieth birthday. Kluwer Academic Publishers, 1996.

[6] Grue, J. and Biberg, D., Wave forces on marine structures with small speed in water of restricted depth. *Appl. Ocean Res.* **15**, 1993, 121-135.

[7] Grue, J. and Palm, E., The mean drift force and yaw moment on marine structures in waves and current. *J. Fluid Mech.* **250**, 1993, 121-142.

[8] Grue, J. and Palm, E., Wave drift damping of floating bodies in slow yaw motion. *J. Fluid Mech.* **319**, 1996, 323-352.

[9] Malenica, S., Clark, P.J. and Molin, B., Wave and current forces on a vertical cylinder free to surge and sway. *Appl. Ocean Res.* **17**, 1995, 79-90.

[10] Newman, J.N., *Marine hydrodynamics.* The MIT Press, 1977.

[11] Newman, J.N., Wave-drift damping of floating bodies. *J. Fluid Mech.* **249**, 1993, 241-259.

[12] Newman, J.N. and Lee, C. H., Sensitivity of wave loads to the discretization of bodies. *Proc. 6th Int. Conf. Behaviour of Offshore Structures (BOSS '92)*, London, U.K., ed. M. H. Patel and R. Gibbins, Vol. 1, BPP Technical Services Ltd., 1992.

[13] Nossen, J., Grue, J. and Palm, E., Wave forces on three-dimensional floating bodies with small forward speed. *J. Fluid Mech.* **227**, 1991, 135-160.

[14] Wehausen, J. V. and Laitone, E. V., Surface waves. *Handbuch der Physik* **IX**, 1960.

[15] Wichers, J.E.W. and Sluijs, M.F., The influence of waves on the low frequency hydrodynamic coefficients of moored vessels. *Proc. Offshore Technology Conf., Houston, OTC 3625*, 1979.

[16] Wu, G. X. and Eatock-Taylor, R., The hydrodynamic force on an oscillating ship with low forward speed. *J. Fluid Mech.* **211**, 1990, 333-353.

[17] Zhao, R. and Faltinsen, O.M., Interaction between current, waves and marine structures. *5th Int. Conf. on Num. Ship Hydrodynamics*, Hiroshima, National Academy Press, Washington D. C., 1989.

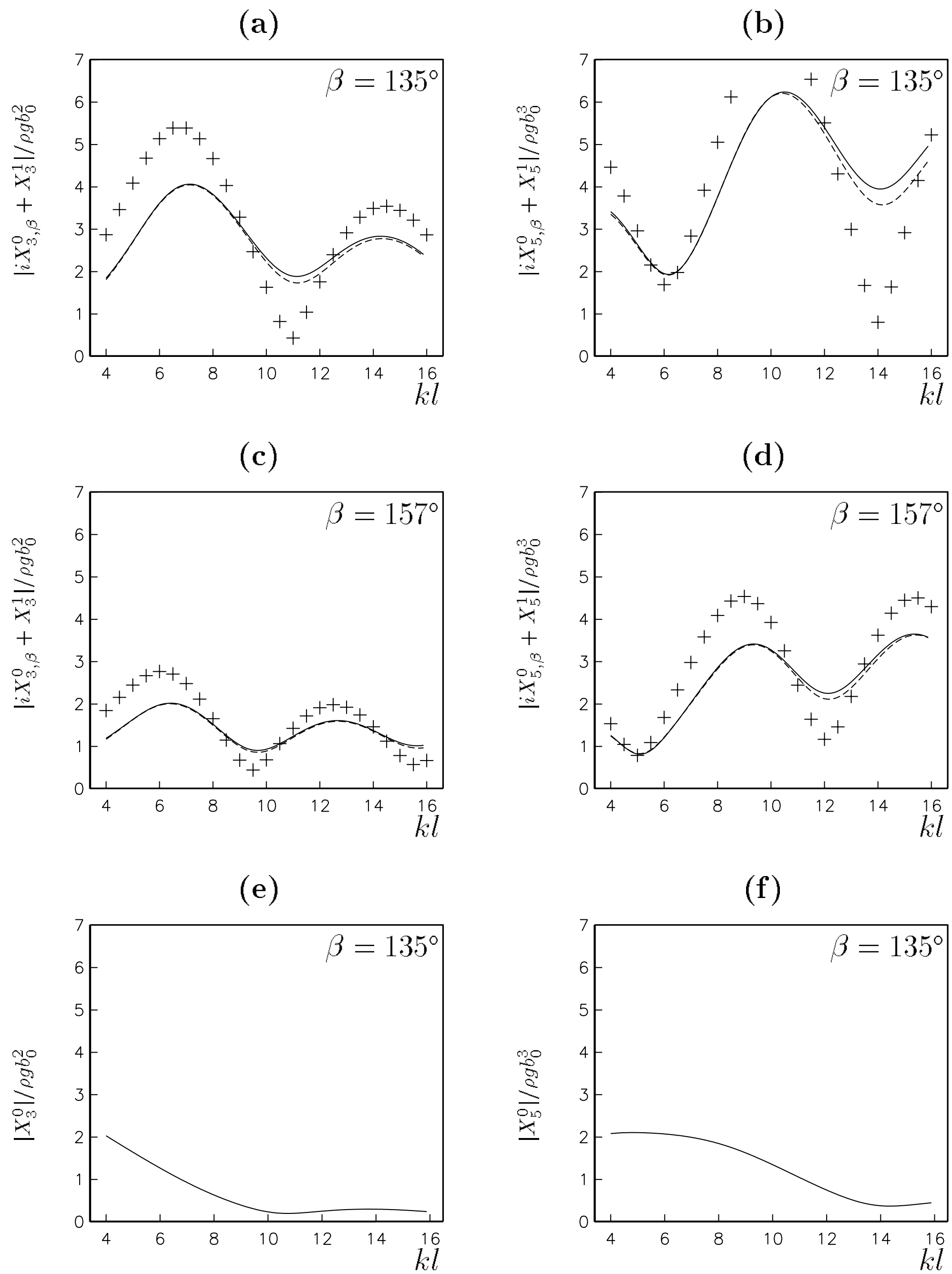

Figure 1: Exciting force in heave and pitch for Ship 1, 3136 panels on S_B and 12544 panels on S_F. Solid line: generalized far-field Haskind relations. Dashed line: pressure integration. Cross marks: $|X_i^1|$ computed by the Haskind relations. In (e) and (f) we have, for comparison, shown $|X_i^0|$. $h = \infty$.

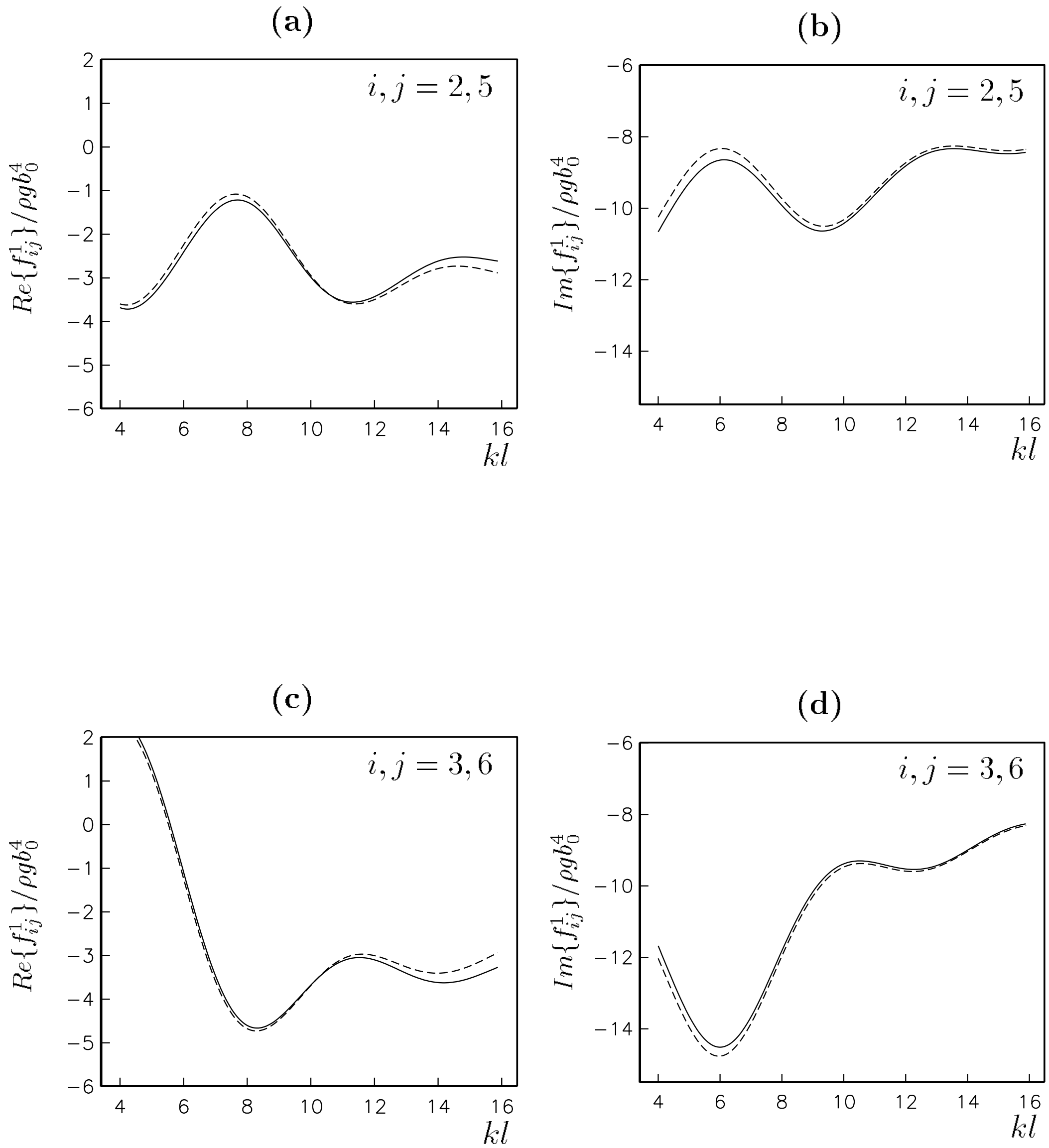

Figure 2: Comparison of f^1_{ij} (solid line) and $-f^1_{ji}$ (dashed line). (a)-(d): Ship 1, 3136 panels on S_B and 12544 panels on S_F.

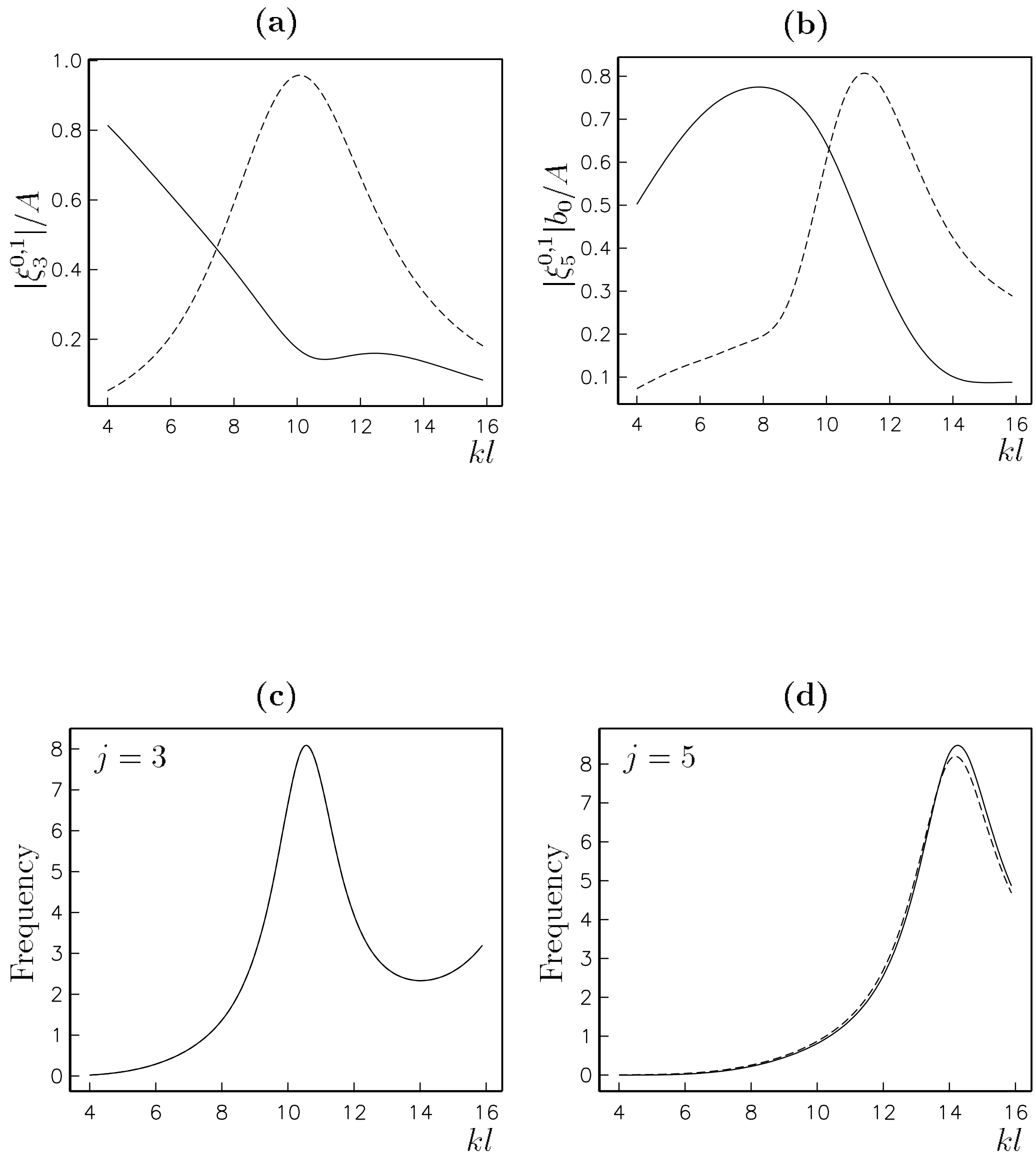

Figure 3: (a) and (b): The body response $|\xi_j^0|$ (solid line), and $|\xi_j^1|$ (dashed line) in heave and pitch. $|\xi_j^1|$ is scaled by a factor 0.1. (c) and (d): The first order frequencies of oscillation $Im\{\frac{1}{\xi_j^0}\frac{\partial \xi_j^0}{\partial \beta}\}$ (solid line), and $Im\{\frac{1}{X_j^0}\frac{\partial X_j^0}{\partial \beta}\}$ (dashed line), also in heave and pitch. All curves are for Ship 1, 1600 panels on S_B and 6400 panels on S_F. $\beta = 135°$. $h = \infty$.

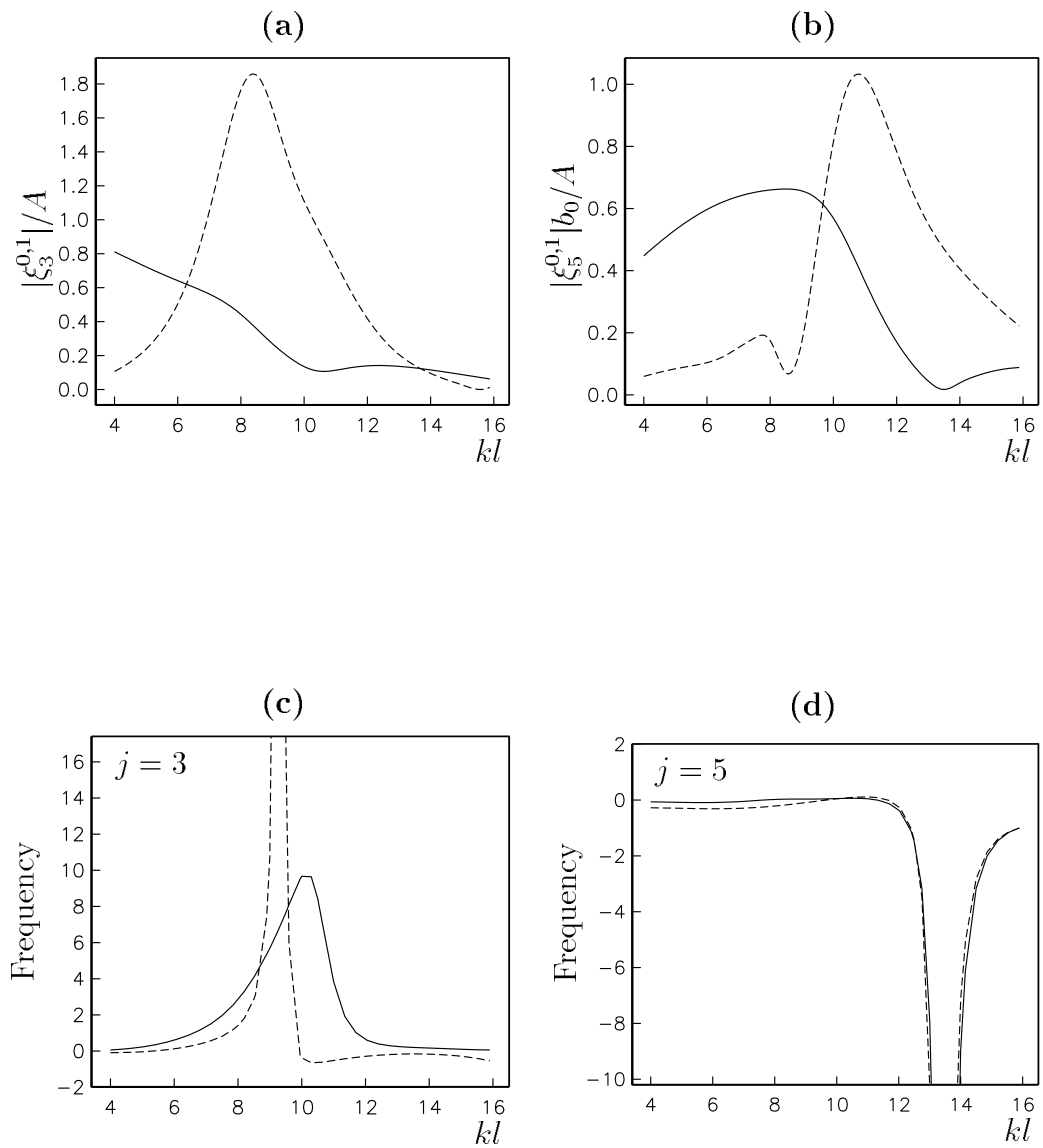

Figure 4: (a)-(d): As Fig. 3, but for the TPS, 760 panels on S_B and 1800 panels on S_F.

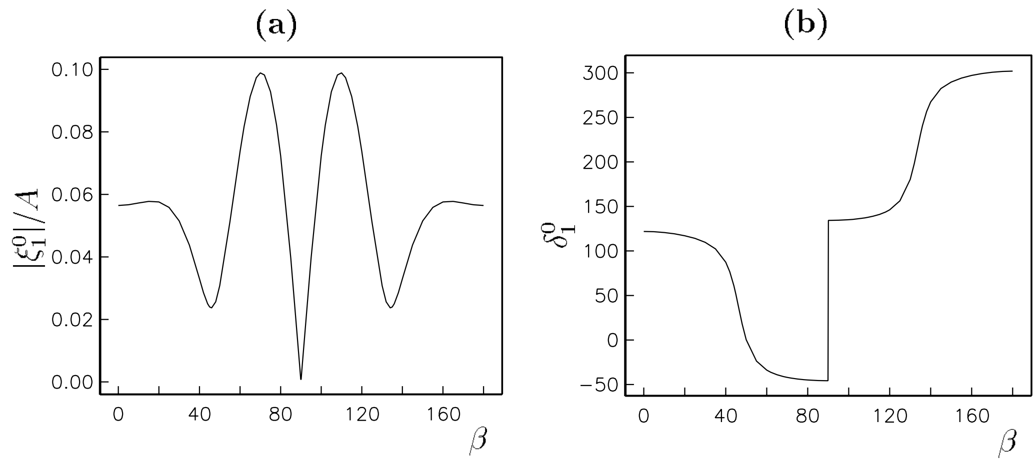

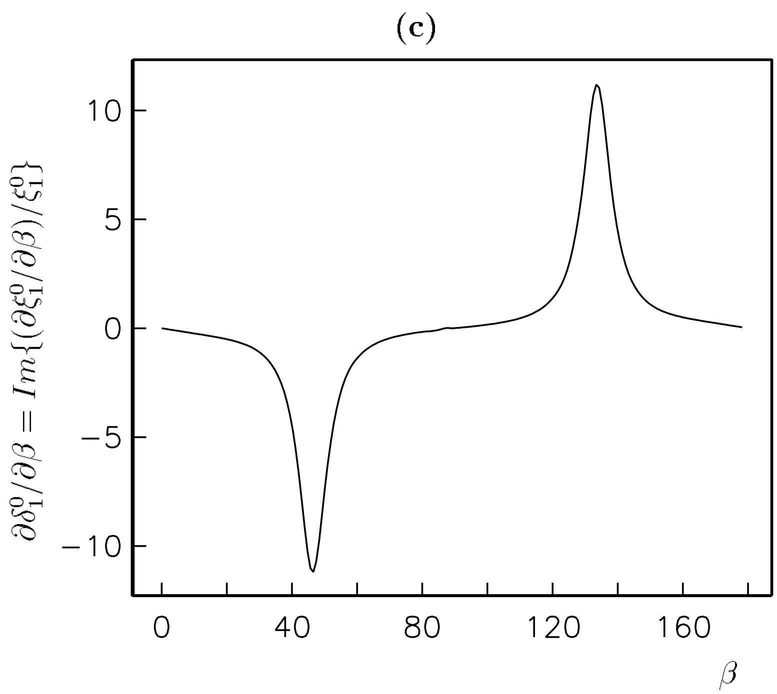

Figure 5: For the surge mode of motion as a function of the wave angle, the figures shows: (a): The body response for $\Omega = 0$. (b): The phase angle. (c): The first order frequency of oscillation. All curves are for Ship 1, 1568 panels on S_B and 6272 panels on S_F. $kl = 12.6$. $h = \infty$.

(a)

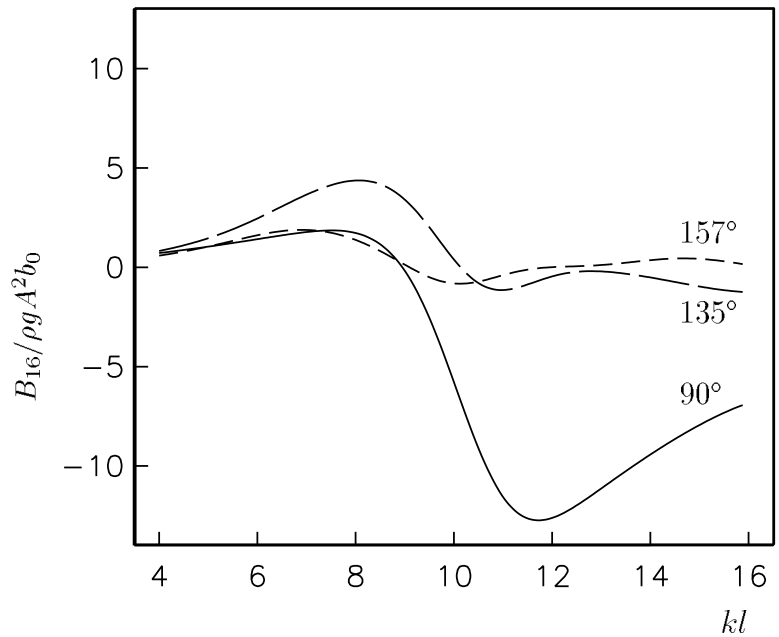

(b)

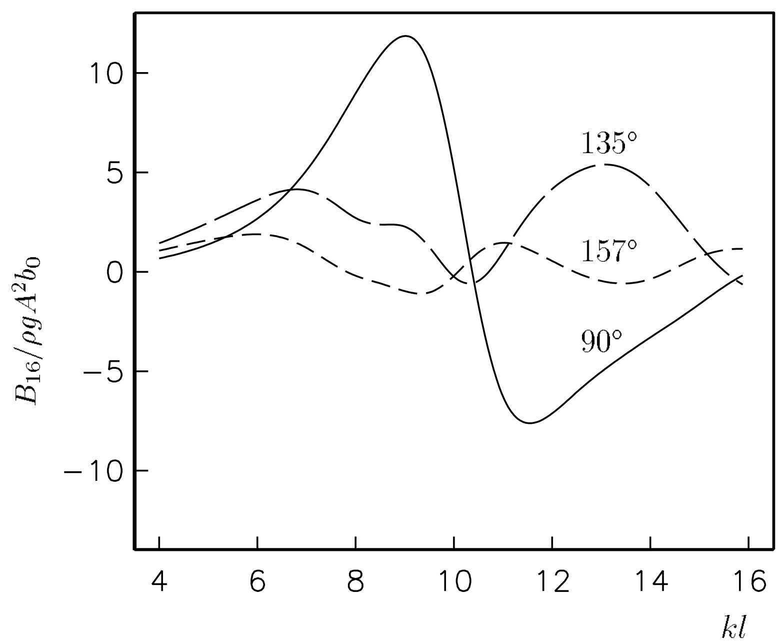

Figure 6: The damping coefficient B_{16} at different wave angles. (a): Ship 1, 1600 panels on S_B and 6400 panels on S_F. (b): The TPS, 760 panels on S_B and 1800 panels on S_F. $h = \infty$.

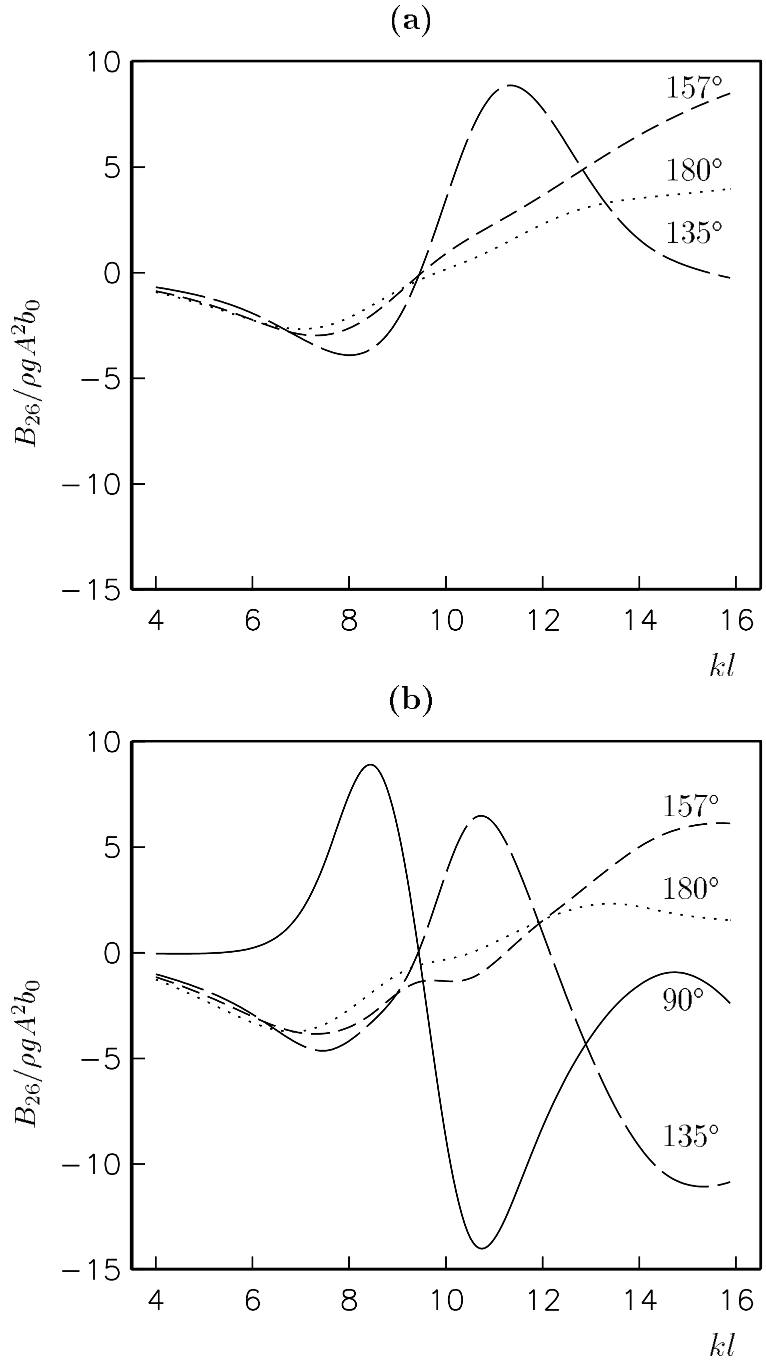

Figure 7: As figure 6, but for B_{26}.

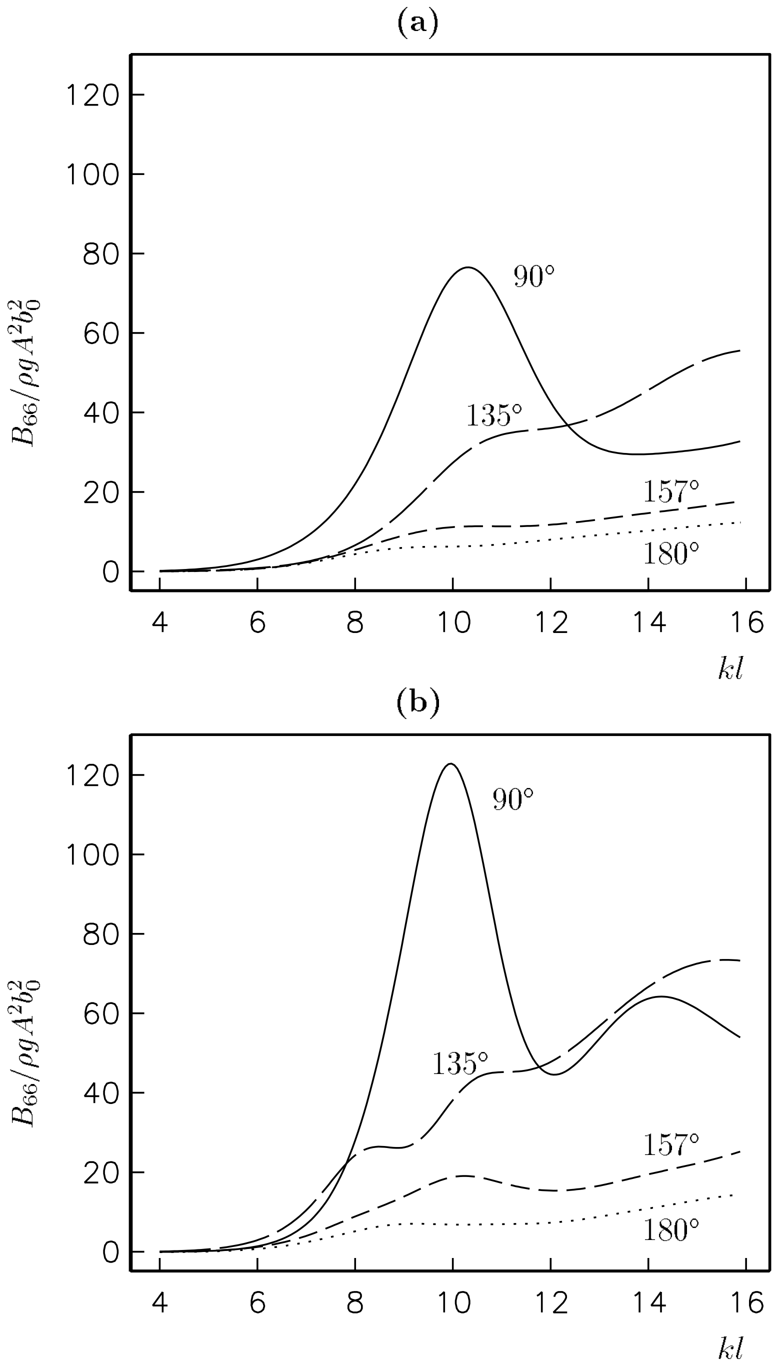

Figure 8: As figure 6 but for B_{66}.

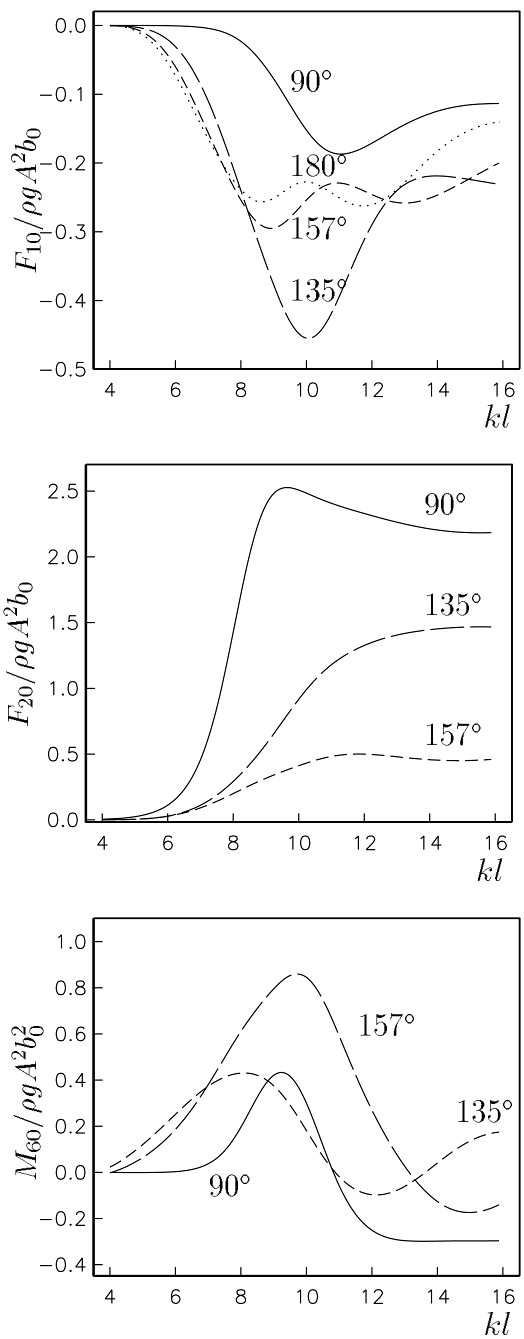

Figure 9: F_{10}, F_{20} and M_{60} at different wave angles. (180° means head waves.) The TPS, 760 panels on S_B. 1800 panels on S_F.

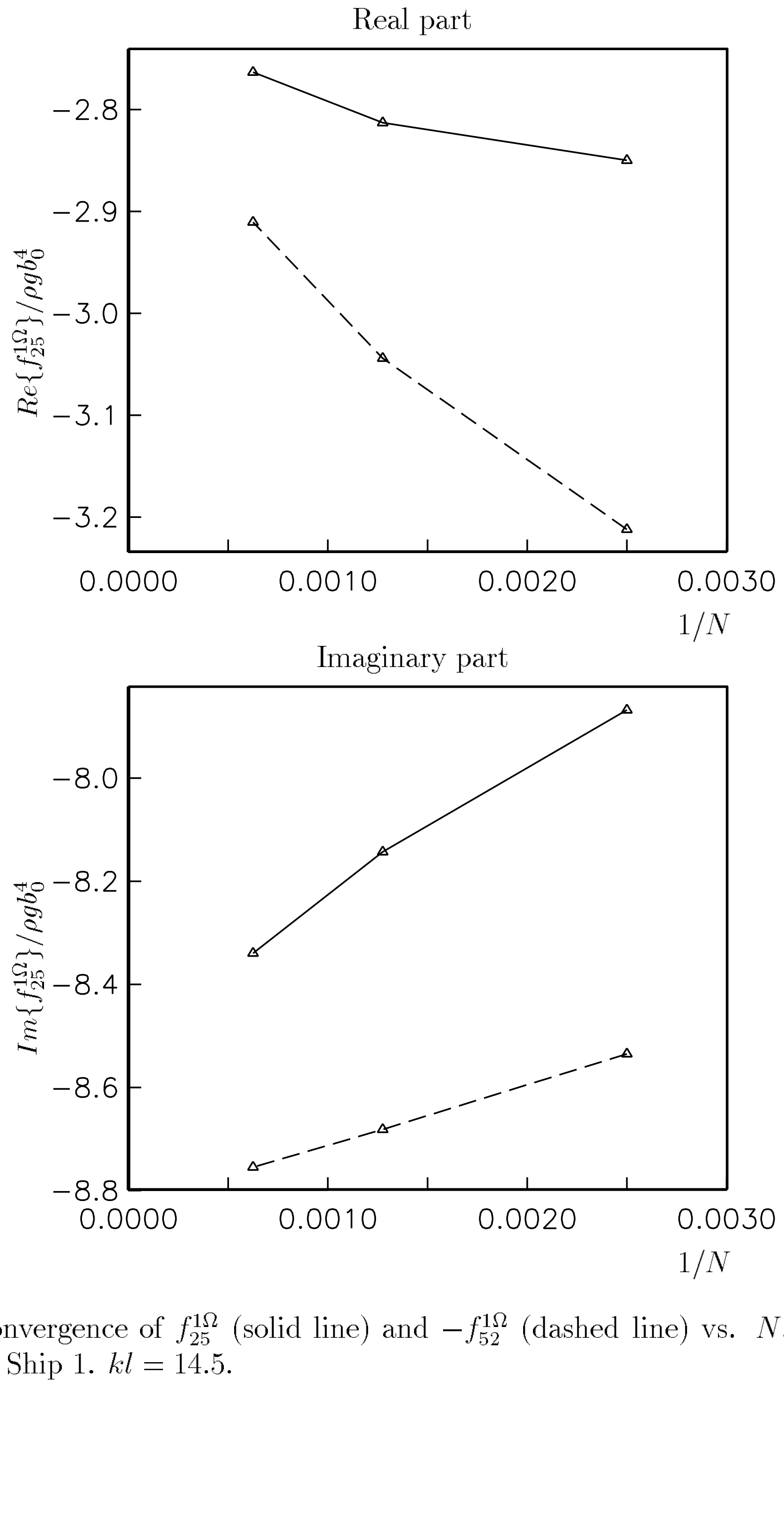

Figure 10: Convergence of $f_{25}^{1\Omega}$ (solid line) and $-f_{52}^{1\Omega}$ (dashed line) vs. N, the number of panels on S_B. Ship 1. $kl = 14.5$.

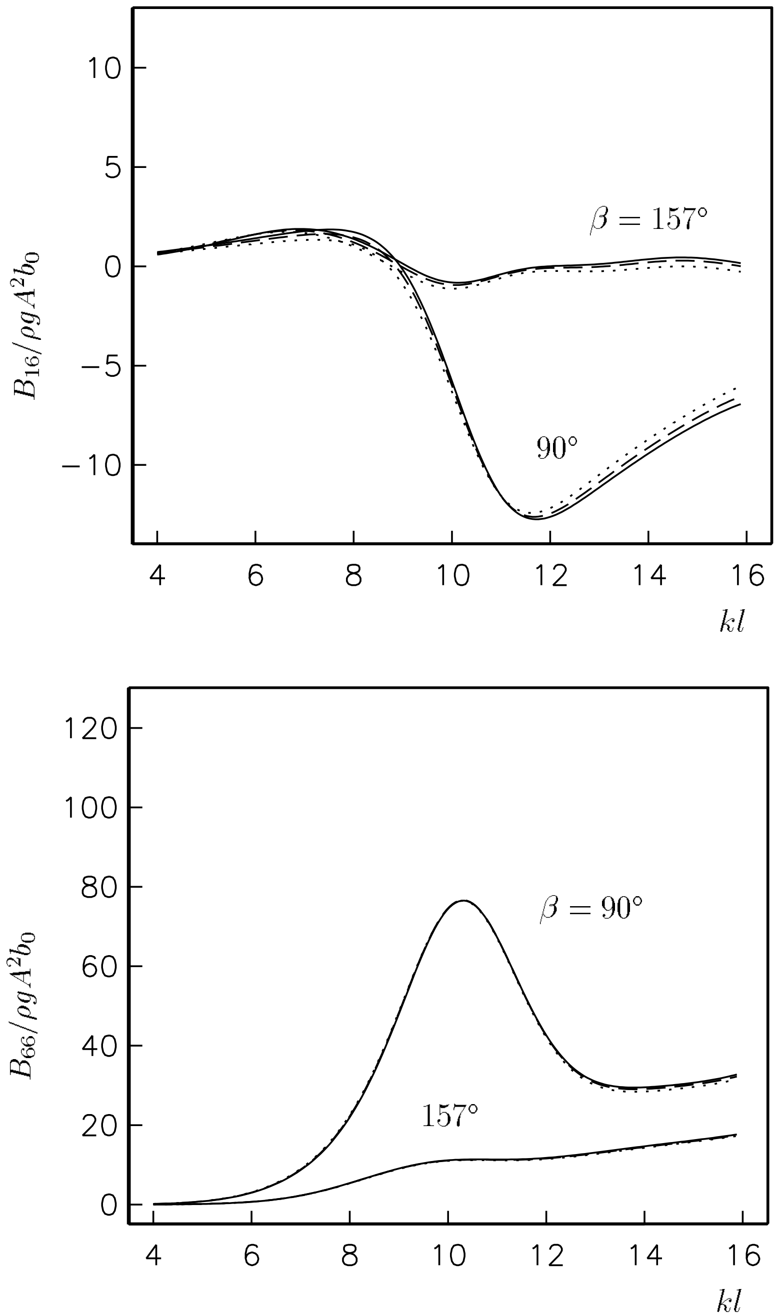

Figure 11: Convergence of B_{16} and B_{66} for Ship 1. Number of panels: Solid line: 1600 on S_B, 6400 on S_F. Dashed line: 784 on S_B, 3136 on S_F. Dotted line: 400 on S_B, 1600 on S_F. $h = \infty$.

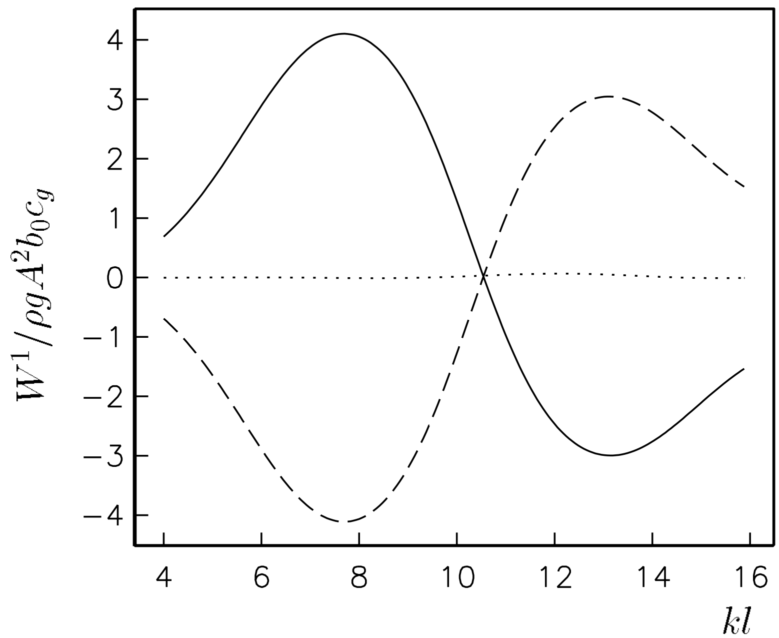

Figure 12: Contribution to the expression for W^1 (eq. (146)) for Ship 1, 1600 panels on S_B and 6400 panels on S_F. Solid line: The far field term. Dashed line: The remaining term. Dotted line: The whole expression. $h = \infty$.

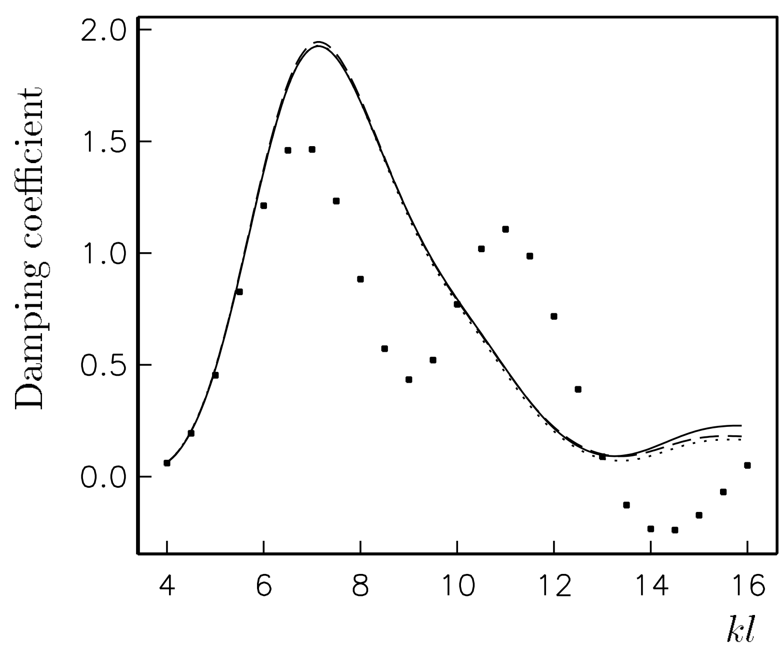

Figure 13: Comparison of the wave drift damping coefficients B_{11}, B_{16} and B_{66} for Ship 1, 1568 panels on S_B,S_F. The ship is moving as described in §8. Head waves. Solid line: $B_{11}/\rho g A^2 b_0$. Dashed line: $B_{16}/\rho g A^2 s K b_0$. Dotted line: $B_{66}/\rho g A^2 s^2 K b_0$. Black squares: $B_{11}/\rho g A^2 b_0$ computed from Aranha's formulae. $h = \infty$.

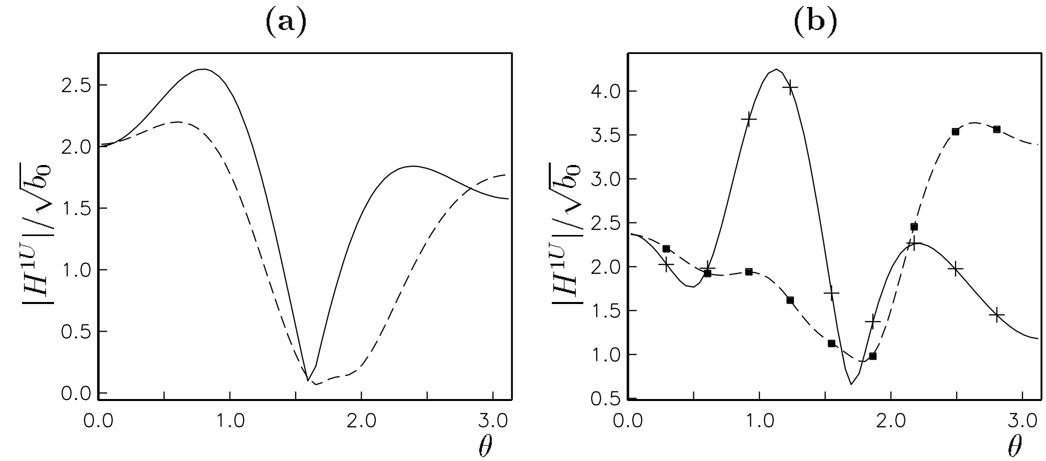

Figure 14: The far-field amplitude function H^{1U} for Ship 1 in translatory motion vs. polar angle θ, $(0 < \theta < \pi)$, computed by complete theory (solid line), and Aranha's formulae (dashed line). Head waves. $h = \infty$. Computations with 1600 panels on S_B, 6400 on S_F. Computations with $N_B = 784$, $N_F = 3136$, are indicated with cross marks (complete theory), and black squares (Aranha's formulae). (a): $kl = 6$. (b): $kl = 8$.

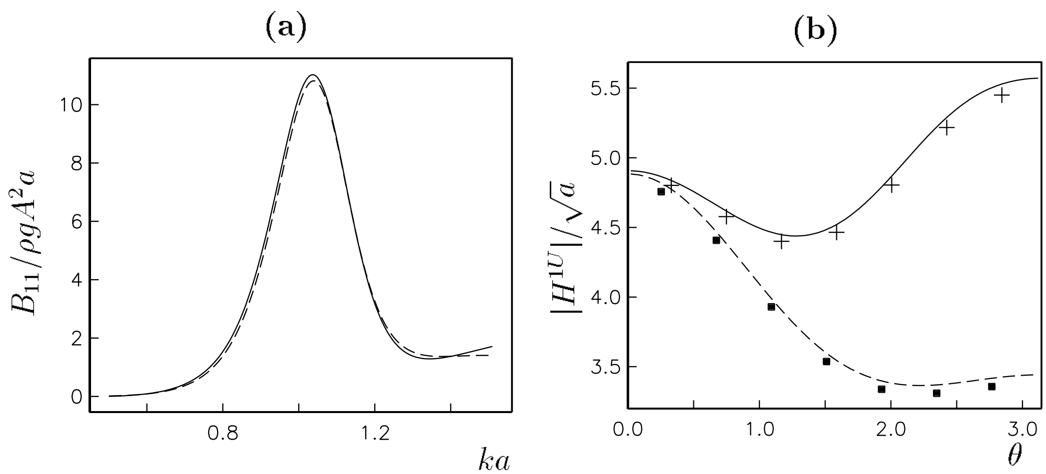

Figure 15: For a half immersed sphere with diameter $2a$, 784 panels on S_B and 1792 panels on S_F, in head waves, the figures show: (a): B_{11} and (b): The far-field amplitude function H^{1U} for translatory motion vs. polar angle θ at $ka = 0.9$. Complete theory (solid line), Aranha's formulae (dashed line). $h = \infty$. Computations with $N_B = 400$, $N_F = 880$, are indicated with cross marks (complete theory), and black squares (Aranha's formulae).